UNIVERSITÀ DEGLI STUDI DI SALERNO

Dipartimento Di Medicina, Chirurgia E Odontoiatria

"Scuola Medica Salernitana"

Corso di Dottorato

in

Medicina Traslazionale dello Sviluppo e dell'Invecchiamento Attivo

XXXV CICLO

Tesi di Dottorato

Therapeutic potentials of the BPIFB4 protein and its Longevity Associated Variant (LAV) in senescence related conditions and its role in platelet function.

Coordinatore:

Ch.mo Prof.

Palmiero Monteleone

Tutor:

Ch.mo Prof.

Annibale Alessandro Puca

Co-Tutor:

Ch.ma Prof.ssa

Elena Ciaglia

Candidato:

Francesco Montella

Matr.: 8800900047

ANNO ACCADEMICO 2021/2022

TABLE OF CONTENT

- Discussion

Chapter V – Platelets express the BPIFB4 protein and contribute to the functional effects of the LAV-BPIFB4 polymorphic variant

- Introduction
- Results
- Materials and Methods
- Discussion

Conclusion

Bibliography

Abstract

Recent studies have demonstrated that the longevity-associated variant (LAV) of bactericidal/permeability-increasing fold-containing family B-member-4 (BPIFB4) protein promotes health and longevity, by enhancing the vascular cell homeostasis, revascularization after ischemic injury, and largely counterbalancing age-related impairments of the immune system and cardiovascular system. These findings helped us to partially explain the health status of Long-Living-Individuals (LLIs) and their homozygous genotype enrichment for LAV-BPIFB4. The levels of circulating BPIFB4 may have an influence on the composition of monocytes and macrophages and may shift the balance toward an anti-inflammatory status. An association was found between non-classical CD14+CD16++ monocyte counts, which are precursors of M2 macrophages with immunomodulatory functions, and LLIs' state. During the ageing process, systemic aging is driven by the senescent immune system, which could be a key therapeutic target to prevent the pathological consequences of aging and extend longevity. Several data show a new senotherapeutic action of LAV-BPIFB4 that may offer a valuable therapeutic tool to control aging and reduce its pathophysiological disorders, such as CVDs or, in senescent GBM cells, enhancement of their sensitivity to temozolomide and a selective reduction of the T cells’ senescence from GBM patients. As a result of its pleiotropic effects on both immune compartments and cellular homeostasis, LAV-BPIFB4 may represent an attractive candidate for developing a new treatment for HD. Indeed, when compared to normal

STHdh Q7/7 cells, STHdh Q111/111 cells were unable to induce pro-resolving microglia phenotype, but LAV-BPIFB4 transduction promptly restored the central immune control through a mechanism involving the CXCR4 axis. Since platelets are primary mediators in innate immune response and combat infection, it was researched the role of this blood figurative elements in immunomodulatory processes of the BPIFB4 protein.

Introduction

Cellular senescence is a condition in which the cell is no longer subject to proliferation, characterized by resistance to apoptosis and loss of physiological function. There are multiple causes of this condition but they are all related to DNA damage or malfunction[1,2]. Cellular senescence has many consequences. As an organ accumulates senescent cells, its function is compromised and aging occurs. It can also be a cause of chemo-resistance to cancer therapy, and it can also induce damage or dysfunction in healthy tissues through the SASP (Senescence Associated Secretory Phenotype). SASP is a collection of chemokines, cytokines, matrix remodeling proteases, and extracellular vesicles (EVs), has been hypothesized to link cellular senescence and inflammaging, and to participate in tissue dysfunction[3,4].

In elderly individuals, the chronic accumulation of senescent cells contributes to tissue dysfunction and increased risk of developing age-related diseases. However, the reduction of senescent cells with various therapeutic approaches may improve health span in elderly individuals[5].

In this context takes apart the protein bactericidal/permeability-increasing fold-containing-family-B-member-4 (BPIFB4) and its Longevity Associated Variant (LAV). BPIFB4 is a secreted protein that has been identified on a genome wide association study, in an Italian set of long-living individuals (LLIs) and controls. Compared to elderly people, LLIs represent a model of successful healthy aging. They are less prone to be affected by CVDs thanks to their ability in preserving both

immune response and inflammatory balance, which are usually lost and/or deteriorated in the elderly[6]. The homozygous genotype showed a clear correlation with high eNOS phosphorylation in serine 1177 that correlates with high activity and Nitric Oxide (NO) production in PBMCs of healthy subjects. Furthermore, an inverse correlation of the homozygous LAV-BPIFB4 was found with frailty in elderly subjects and accordingly, in old mice LAV-BPIFB4 gene transfer delayed frailty progression[7]. BPIFB4 is a secreted protein found in respiratory secretion, upper airways and proximal trachea[8] with an appreciable expression also in cardiomyocytes and endothelial cells[9], PBMCs[10], cardiac pericytes (personal communication) and striatal-derived cell lines[11]. BPIFB4 is particularly abundant in serum of long-living individuals presumably allowing them to maintain a proper balance between anti-inflammatory and proinflammatory mechanisms without encountering the detrimental remodeling of immune system usually found in the elderly[12]. Here it will discussed the role of the LAV haplotype in the BPIFB4 gene in restoring the proper inflammatory balance and successfully modulating the immune system in physio-pathological conditions directly (or indirectly) related to senescence.

Aims of Project

The rise in average life expectancy leads to the onset of chronic pathological states, for which new resources and knowledge are needed in order to improve the quality of life of subjects in the third age. This research project is based on the study of a protein that appears to be associated with longevity, lower endothelial fragility and improved cardiovascular function and aims to investigate its influence on the immune system. Considering the influence of LAV-BPIFF4 on the immune system, the research project focused on the effects of the protein in the phenomenon of senescence and related or consequent pathologies. Understanding the low frailty of long-lived individuals, the biological mechanism of the reparative and/or conservative effect at the endothelial level can be useful in order to obtain a clearer picture of the functions of this protein with the aim of increasing knowledge useful for improving the quality of life and speeding up intra- and post-hospital recovery.

The research plan covered a period of about three years combining proteomic techniques, cytofluorimetric analysis and in vitro assays. Although related to senescence and the immune system, the pathological contexts addressed are different from each other. A first approach has been the study of the influence of the protein on monocytes pool and macrophages skewing, shifting the balance toward an anti-inflammatory phenotype. Subsequently, were outlined the effects on the deleterious age-related changes of the immune system and thereby the senescence-associated events. An other pathological context was also studied, not

directly related to the immune system or senescence, such as neurodegeneration, using a Huntington's model. Since the LAV-BPIFB4 protein is present in soluble form in the circulatory system, the study was focused on platelets as a putative vehicle of the protein and mediator of the immunological effects.

This research project, with these many tasks, has added other important pieces for demonstrating the importance of the pleiotropic effects of the protein.

Chapter I – Circulating BPIFB4 influences the abundance of reparative monocytes and macrophages in LLI

Elena Ciaglia, **Francesco Montella**, Valentina Lopardo, Pasqualina Scala, Anna Ferrario, Monica Cattaneo, Albino Carrizzo, Alberto Malovini, Paolo Madeddu, Carmine Vecchione and Annibale Alessandro Puca. *Circulating BPIFB4 Levels Associate With and Influence the Abundance of Reparative Monocytes and Macrophages in Long Living Individuals.* **Front Immunol. 2020 May** 29;11:1034. Doi: 10.3389/fimmu.2020.01034.

Introduction

In developed countries, life expectancy averages 78 for males and 83 for females (1), but some unique individuals prolong aging and live much longer than the rest of the population. Long Living Individuals (LLIs) symbolize a model of optimistic biology and an special resource to study and find a way to enhance general public health. Investigation of extended healthy aging could direct to important interpretation on systems that protect from age related diseases [(1)]. Chronic inflammation is related with shorter life expectation [(2)] and with diseases that decrease the quality of life of aged people (termed inflammaging) [(3)]. Several indicators have been proposed to trace systemic and vascular inflammation [(4)], but none has been developed yet to shed light on the opposite aspect of that subject.

Results

Long-Living Individuals (LLIs) delay aging and are less prone to chronic inflammatory reactions. It was hypothesize that BPIFB4 may influence monocytes pool and macrophages skewing, shifting the balance toward an anti-inflammatory phenotype. It was profiled circulating monocytes in 52 LLIs (median-age 97) and 52 healthy volunteers (median-age 55) using flow cytometry. Even if the frequency of total monocyte did not alter, the intermediate CD14++CD16+ monocytes counts were lower in LLIs evaluated to control adults. On the other hand, non-classical CD14+CD16++ monocyte counts, which are M2 macrophage precursors with an immunomodulatory function, were found significantly related with the LLIs' state. In a differentiation assay, supplement of the LLIs' plasma improved the ability of

monocytes, either from LLIs or controls, to get a paracrine M2 phenotype. A neutralizing antibody versus the phosphorylation site (ser 75) of BPIFB4 reduced the M2 skewing outcome of the LLIs' plasma.

Before starting the characterization of monocytes in LLIs, an ELISA assay for the circulating BPIFB4 protein was performed in the plasma of donors, subdivided by age, and long-lived donors, as shown in Fig1.1A. The characterization of monocytic dynamics in long living individuals (LLIs) it was performed with an analysis of monocytes frequency in LLIs (median age 97, range 95–99, N = 52) expressed by percentage of total CD14+ positive cells using cytofluorimetric analysis. Control group is subdivided in adults (35–45 years, n = 18) and old volunteers (65–75 years, n = 24) (Fig.1.1 B-C-D). The strategy gating was executed as shown in Fig.1.1B, representative FACS gates displaying the relative abundance of different monocyte cell subsets based on the expression of CD14+ and CD16+ markers among freshly isolated PBMC from control volunteer (left plot, 67 years-old male) vs. LLI (right plot, 98 years-old male). Flow-cytometry data indicate a particular distribution of the monocyte pool, which uniquely marks LLIs (Fig 1.1). Regarding the total circulating monocyte population, it was observed no significant variation ($P < 0.05$) in LLIs compared with controls (Fig 1.1C). Next, a particular subsets of monocytes were considered: CD14+CD16++ non-classical monocytes where were significantly increased in LLIs compared to young and old controls (Fig 1.1D, $P < 0.001$).

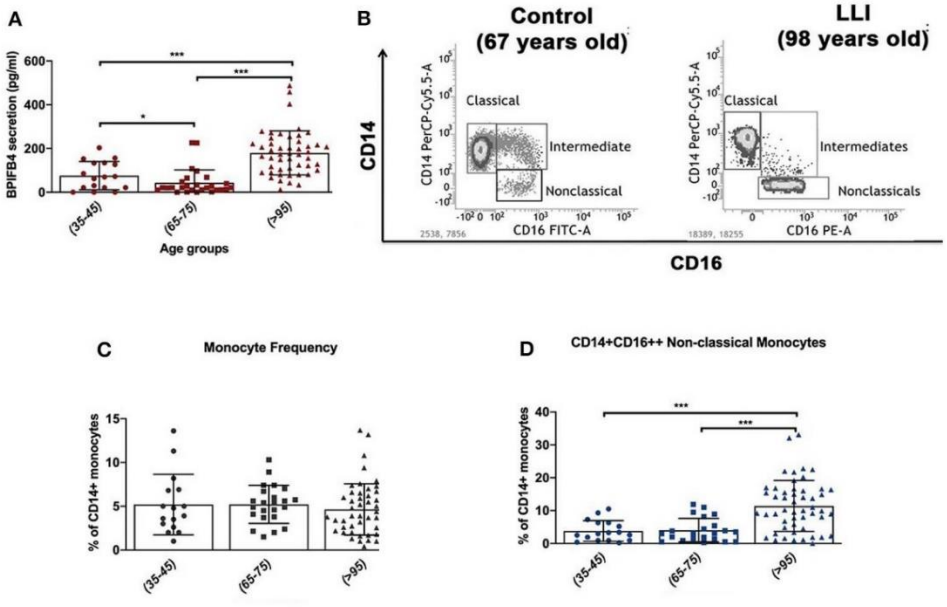

Figure 1.1 Analysis of circulating monocytes and their subset.

It was then examined whether the plasma of LLI could influence the monocyte-derived macrophage phenotype towards the pro-resolving M2 (alternatively activated) or pro-inflammatory M1 phenotype. Macrophages were generated from peripheral blood monocytes of controls (35–75 years, N = 10) and of long living individuals (range 95–99, N = 10) upon 7 days in vitro culture with 20% autologous plasma. As reported in Fig 1.2A, control macrophages manifested an M1-M2 intermediate profile presenting the canonical CD206+/CD163–/CD80low phenotype. Instead, LLIs' macrophages showed an enhancement M2 phenotype as indicated by higher surface level of both CD206 and of the anti-inflammatory marker CD163 (Fig 1.2A,B). Knock-down of BPIFB4 or mutagenesis of protein is known to reduce the BPIFB4 ability to sustain endothelial function. To verify if BPIFB4 is dependable for the ability of the LLIs' plasma to promote M2 polarization of monocytes it was used a blocking antibody. Interestingly, the BPIFB4-neutralizing antibody produced a substantial reduction in macrophage M2 (CD206+/CD163+) recovery (Fig 1.2C,D) upon stimulus with LLIs' plasma.

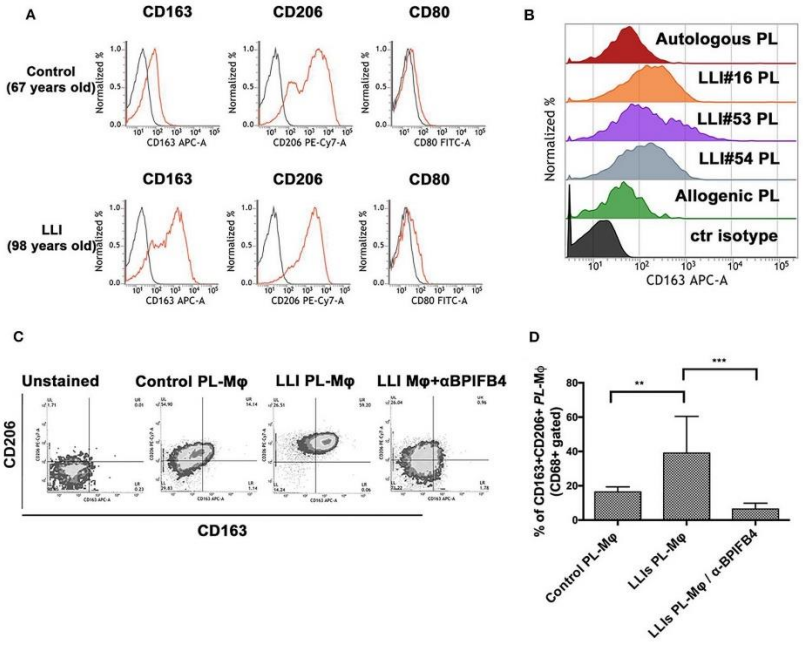

Figure 1.2 In vitro conditioning with plasma from long living individuals leads to polarization of LLIs and controls macrophages toward M2 phenotypes

Methods

Patients Recruitment

The study was executed on a set of 104 individuals: n = 52 control volunteers (median age 55, range 35–75) and n = 52 long-living individuals LLIs (median age 97, range 95–99). Control volunteers group was divided in middle-aged (35–45 years) and old(er) group (65–75 years). These were constituted, respectively, by healthy donors and by subjects with no apparent diseases who underwent routine preventive laboratory tests. For each, venous blood (10mL) was withdrawn for analyses and detailed anamnesis was collected. For detailed information concerning LLIs group see Table 1. All participants signed an informed consent for the management of personal anamnestic data and blood samples. The study was approved by the IRCCS MultiMedica ethical committee and conducted in accordance with the ethical principles deriving from the Declaration of Helsinki.

CD14+ Monocytes Isolation and Macrophage Generation

Peripheral Blood Mononuclear Cells (PBMC) were separated from whole blood by density gradient (Ficoll). After separation, PBMC were collected and washed for the subsequent experiments. CD14+ monocytes were positively selected from PBMCs by an immunomagnetic procedure (Miltenyi Biotec). Then, CD14+ cells were induced to differentiate in M1 or M2 macrophages using reagents included in the CellXVivoTM Human M1 or M2 Macrophage Differentiation Kit (R&D system), or alternatively in the presence of 20% human plasma (MPL). Monocytes stimulated with plasma were cultured in serum free base media (R&D system) with or without BPIFB4 blocking antibody. Blocking antibody for BPIFB4 was bought from CliniSciences S.r.l.-Guidonia Montecelio—Italy. All cell cultures were conducted at 37C◦ in humidified 5% CO2 atmosphere.

Antibodies and Flow Cytometry

Single-cell suspensions were stained with mAb against human CD14 (HCD14; BioLegend; 1:20), CD16 (REA423; Miltenyi Biotec GmbH; 1:50), CD206 (DCN228; Miltenyi Biotec GmbH; 1:11), CD163 (REA812; Miltenyi Biotec GmbH; 1:50), CD68 (Y1/82A; BioLegend; 1:20), CD80 (2D10; BioLegend; 1:20). After 20min incubation at 4◦C in the dark, cells were washed and resuspended in PBS for the FACS analysis. For each test, cells was analyzed using FACS Verse Flow Cytometer (BD Biosciences).

ELISA

Plasma concentrations of BPIFB4 were assessed using ELISA Kit (Cusabio CSB-YP003694HU) following the manufacturer’s protocol.

Statistical Analysis

In all other experiments shown, statistical analysis was performed by using the GraphPad prism 6.0 software for Windows (GraphPad software). For each type of assay or phenotypic analysis, data obtained from multiple experiments are calculated

as mean ± SD and analyzed for statistical significance using ANOVA for multiple comparison $p < 0.05$ were considered significant. $*p < 0.05$, $**p < 0.01$, and $***p < 0.001$.

Discussion

The enriched subclass of non-classical monocytes is known to dynamically *patrol* the vasculature and eliminate damaged cells in numerous disease conditions, in that way supporting tissue healing and the resolve of inflammation [(5)]. The model of "patrolling monocytes" (PMo) initially referred to mouse (Ly6Clow) rather than human cells (CD14+CD16++). Circulating concentrations of PMo often reflect their penetration within the parenchyma of numerous tissues in most of age-related diseases, including cardiovascular diseases, stroke, neurological damage, arthritis. In myocardial infarction, patrolling monocytes have been related with reparative, pro-angiogenic, and pro-arteriogenic effects [(6)]. Collecting evidence suggests non-classical patrolling monocytes might operate as the main precursor for tissue resident macrophages or as precursors for alternatively activated macrophages during inflammation. In fact non-classical monocytes have been observed to differentiate into protective M2- macrophages during low tissue injury [(7)].

Even if the associative description of data does not allow to conclude the skewed monocyte profile is significant to the prolonged health-span of the studied LLIs, this data represents the first study to describe a major monocyte subset in people that reach extreme ages (>95 years). M2 macrophages have a role in defending from many diseases related with aging. So, a reasonable scenario emerging from this study is that high levels of circulating BPIFB4 support M2 polarization thereby creating an innate immunity background supportive to disease resistance and control of inflammatory responses.

Chapter II – Reduction of $CD38^+$ macrophages and NAD^+ decline after BPIFB4 gene infection

Ciaglia E, Lopardo V, **Montella F**, Carrizzo A, Di Pietro P, Malavolta M, Giacconi R, Orlando F, Cattaneo M, Madeddu P, Vecchione C, Puca AA. *Transfer of the longevity-associated variant of BPIFB4 gene rejuvenates immune system and vasculature by a reduction of CD38+ macrophages and NAD+ decline*. **Cell Death Dis. 2022 Jan** 27;13(1):86. Doi: 10.1038/s41419-022-04535-z. PMID: 35087020; PMCID: PMC8792139.

Introduction

During aging, there is a increasing deficiency of cellular homeostasis that make organs less competent and more vulnerable to stressors. An example is the age-related regression of the immune system (termed immunesenescence) that becomes less efficient in surveying and defending the organism from inflammatory environments (inflammaging), thus providing to the organism ageing [(1)]. Seeking causal dynamics in driving aging, the amount of NAD+, the well-known nucleotide regulatory cellular homeostasis, decreased during aging and in progeroid disorders, contributing to metabolic dysfunction and a deterioration in overall fitness [(2)]. In recent times, the influence of the senescent immune system to systemic aging has come out. Indeed, immune cells suffering senescence show a peculiar senescence-associated secretory phenotype (SASP), can drive the loss of tissue homeostasis, damage, and age-associated changes in several peripheral organs, thus contributing to reduced lifespan [(3)]. A potential mechanistic association among senescent cells (SnC), inflammation, and the decline of NAD+ in vivo during aging was recently recognized in the NAD glycohydrolase CD38 [(4)]. Regarding the protein LAV-BPIFB4, it showed the potential to drive a macrophage-polarizing outcome toward a pro-resolving M2 phenotype in atherosclerotic patients[(5)] and to redirect peripheral monocyte differentiation into regulatory dendritic cells that can counteract the low-grade chronic inflammatory state.

Results

A flow cytometric approach has been used to study the effects of systemic adeno-associated virus-mediated LAV-BPIFB4 gene transfer in peripheral blood and lymphoid tissues (bone marrow and spleen) on old mice's immune dynamics. The study was conducted on eight C57BL/6J male mice aged 26 months, who were randomly assigned to two experimental groups: a treatment group with one thousand hundred fourteen viral particles injected intravenously (i.v.) into the tail vein for 60 days (N = 4 mice) and a control group (AAVGFP; N = 4 mice) receiving a similar AAV-GFP injection. On the sixtieth day since the beginning of the infection, the senescence associated β-galactosidase (SA-β-gal) substrate has been used to identify CD45+ and CD11b+ myeloid cells in freshly isolated PBMCs, splenocytes, and bone marrow (BM)-derived cells to determine cellular senescence in these cells. As control, N = 5 young (4-months-old) C57BL/6J male mice were also analyzed. The activity of SA-beta Gal was increased in peripheral blood mononuclear cells of aged mice, as expected (Fig. 2.1A). This increase is most significant in CD11b+ myeloid cells (Fig. 2.1B). Remarkably, 60 days of AAV-LAV-BPIFB4 infection followed in a significant reduction in senescent pool of peripheral immune cells and a simultaneous enrichment of senescent cells in the spleen of AAV-LAV-BPIFB4 mice evaluated to old-GFP-mice.

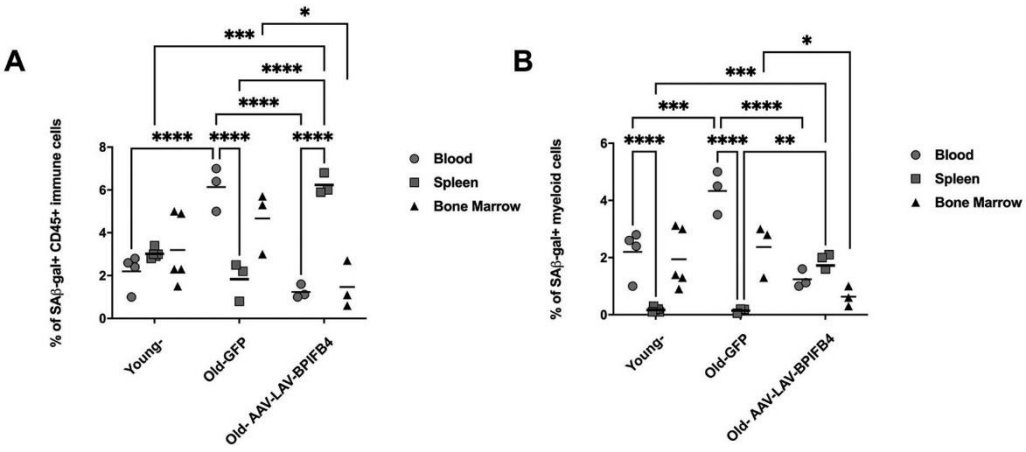

Figure 2.1 Senescence associated β-galactosidase analysis in immune cells

In particular, observed senescence in immune cells may be sufficient to transfer and/or maintain senescence in a manner causing SASP-mediated damage in other [4]. Next, to demonstrate this effect, it was also quantified the aging of aortas in young GFP and AAV-LAV mice. As expected, SA-β-Gal staining of aortas in aged mice resulted in a robust induction of aging-associated immunoreactivity compared with young mice; In contrast, SA-β-gal-positive areas were significantly reduced in AAV-LAV-treated mice compared with the aortas of aged mice (Fig. 2.2A). From a functional standpoint, chronic sterile inflammation recently associated with senile aging has been linked to a decline in NAD+ and thus disease states. This prompted us to analyze NAD+ plasma levels in young control mice as well as aged AAV-GFP and AAV-LAV mice. this data document a decrease in NAD+ levels during aging in vivo; as expected, treatment with AAV-LAVBPIFB4 promoted the reversal of the NAD+ decline (Fig. 2.2B).

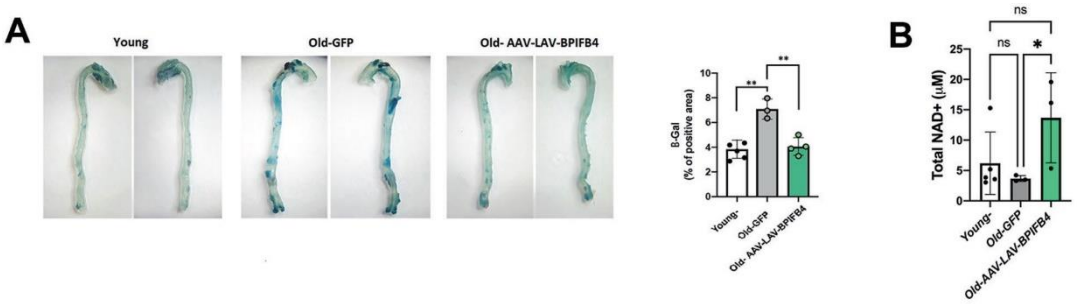

Figure 2.2 Senescence associated β-galactosidase in aorta and total NAD+ analysis

It was further characterized the abundance of CD38+ cells in the blood, bone marrow, and spleen of AAV-LAV-BPIFB4-infected mice compared with AAV-GFP aged mice. Notably, it was found that AAV-LAV-BPIFB4 treatment had no significant effect on circulating CD38+Ly6C+ monocytes (Fig. 2.3A), while a strong decline in CD38+Ly6C+ monocytes (on both Ly6Chigh and Ly6Clow cell subsets) was observed in tissue bone marrow when evaluating AAV-LAV-BPIFB4 aged mice to old AAV-GFP-mice (Fig. 2.3B, C). Likewise, it was observed a reduced accumulation of CD38+Ly6C+ tissue-resident monocytes in the spleen of aged mice

(Fig. 2.3D) and to a better extent than of CD38+Ly6Chigh proinflammatory monocytes was reduced after AAV-LAV-BPIFB4 infection, as compared to those of AAV-GFP-aged mice (Fig. 2.3E).

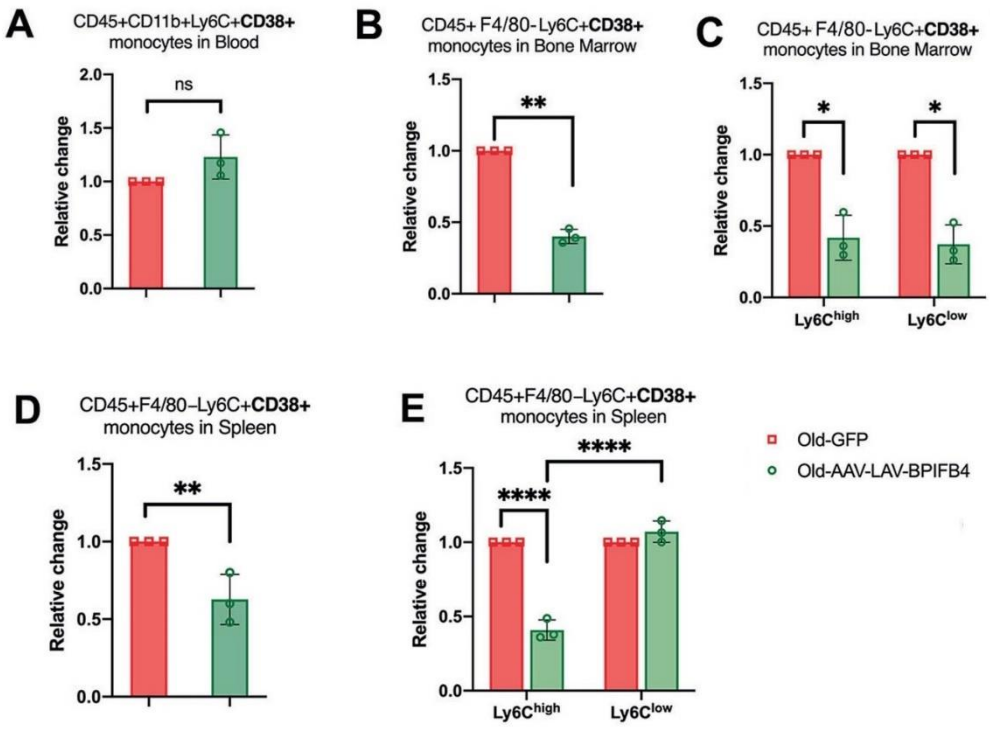

Figure 2.3 Monocytes characterization of phenotype

Methods

Animal models Eight C57BL/6J male mice aged 26 months were randomly assigned to two experimental groups: a treatment group (n = 4 mice; reported as Old-AAVLAV BPIFB4 mice) receiving an intravenous injection (i.v. into the tail vein) of 1*1014 viral particles of AAV-LAV-BPIFB4 60 days earlier and a control group

(n = 4 mice reported as Old-GFP mice) receiving an identical injection of AAV-GFP. Five C57BL/6J male mice aged 4 months were analyzed as a young control group (n = 5 mice; reported as young mice). The animal study was reviewed and approved by the Organismo Preposto al Benessere Animale (OPBA, animal care, and health committee) of IRCCS INRCA, Ancona (Italy), and by the Italian Ministry of Health (authorization n. 130/2018-PR).

Cloning

To obtain BPIFB4 constructs in pAAV2.1 TBG eGFP3 vector, BPIFB4 cDNA was PCR amplified on pRK5 vector with the following primers: AAGCGGCCGCATGCTGCAGCAAAGTGATG for the insertion of NotI site at 5′ end; GCAAGCTTTCATGCGCTCAGCACCAAAAG for the insertion of HindIII site at 3′ end. PCR products were purified with Wizard SV Gel and PCR Clean Up System (Promega), digested with NotI and HindIII, and cloned in pAAV2.1 TBG vector replacing the eGFP. All constructs were sequenced for the BPIFB4 gene.

Mice tissue sampling and processing

Spleen, femur, aortas, and blood were obtained from the mice after the sacrifice. Heparinized blood and plasma were collected. Single-cell suspension from bone marrow and spleen were also harvested for analysis by flow cytometry. Aortas were harvested and placed on a wire system for β-galactosidase staining. Peripheral blood mononuclear cells (PBMCs) were extracted from the whole blood of mice by Ficoll density gradient (Histopaque®- 1077, Sigma-Aldrich) and analyzed by flow cytometry. Spleens were dissociated into single-cell suspension by mechanical digestion. Each spleen was transferred into a sterile 100 mm culture dish containing 10 mL of RPMI-free (Gibco®, ThermoFisher Scientific) supplemented with 2% (v/v) penicillin–streptomycin (Aurogene). Each spleen was pressed using the flat end of a sterile plunger to crush the spleen in circular motions and splenocytes were harvested in a tube to let debris deposit. Cell suspensions were centrifuged at 400 × g for 5 min at RT. After discarding the supernatant, cell pellet was resuspended in a

2 mL Red Blood Cell Lysis Buffer and incubated for 4 minutes on ice. To stop the lysis reaction, 10 mL of PBS was added, and the cell suspensions were centrifuged at 400 × g for 5 min. After discarding the supernatant, cells were assayed for flow cytometry. Bone marrow was extracted from the femur through the flushing method on ice. Femurs were cut at both ends with a sterile blade and bone marrow was flushed out by using a 10 cc syringe filled with RPMI-free (Gibco®, ThermoFisher Scientific) supplemented with 2% (v/v) penicillin–streptomycin (Aurogene). Bone marrow-derived cell suspensions were harvested in a tube to let debris deposit. Cell suspension was transferred in a new tube, centrifuged at 1900 rpm for 5 min at RT. After discarding the supernatant, cells were assayed for flow cytometry

Aortas β-galactosidase staining

To evaluate vascular senescence in the aortic vessels, aortas were fixed for 10 min at room temperature in 2% formaldehyde/0.25% glutaraldehyde solution. Subsequently, vessels were incubated with fresh senescenceβ-galactosidase (SA-β-gal) staining solution (Cell SignalingTechnology) at 37 °C for 24 h and then washed three times with PBS before to be acquired with a digital camera Nikon D300s digital camera. Semi-quantitative analysis of SA-β-gal-positive staining was performed with ImageJ software.

Antibodies and flow cytometry

Single-cell suspensions from murine bone marrow, spleen, PBMCs cells were stained with mAb against mouse CD45 (30F11; Miltenyi Biotec; 1:50), mouse CD11b (M1/70.15.11.5; Miltenyi Biotec; 1:50), mouse Ly-6C (REA796; Miltenyi Biotec; 1:50), mouse F4/80 (BM8; Biolegend; 1:10), mouse CD38 (REA616, Miltenyi Biotec; 1:50), mouse SPiDER- β-Gal (SG03-10; Dojindo Molecular Technologies; 1:500. After 20 min incubation at 4 °C in the dark, cells were washed and resuspended in staining buffer for the FACS analysis. Additional staining for Saβ-galactosidase was performed after the above-mentioned staining and incubated

for 15 min at 37 °C in the dark without washing before FACS analysis. For each test, cells were analyzed using FACS Verse Flow Cytometer (BD Biosciences)

NAD/NADH assay

Total NAD and NADH Assay Kit (Colorimetric) (ab186032) was employed to detect total NAD and NADH plasmatic levels in recruited patients following manufacturers' instructions. 50 µL NAD/NADH reaction mixture were added to 50 µL plasma and incubated at RT up to 2 h. Absorbance was monitored and read with an absorbance plate reader at 460 nm after 1 h and 2 h of incubation.

Statistical analysis

In all experiments shown, statistical analysis was performed by using the GraphPad Prism 9.0 software for Windows (GraphPad software). For each type of assay or phenotypic analysis, data obtained from multiple experiments are calculated as mean ± SD and analyzed for statistical significance using appropriate tests. An analysis of variance (ANOVA) for multiple comparison and followed by post-hoc analysis P values < 0.05 were considered significant; $*P < 0.05$, $**P < 0.01$, and $***P < 0.001$.

Discussion

In vivo data showed that 26-months-old mice had a higher frequency of CD45+SA-beta Gal+ immune cells in blood than young (4-months-old) C57BL/6J mice. Instead, AAVLAV-BPIFB4 gene transfer, in old mice, decreased the pool of peripheral immunosenescent cells that were revealed to be enriched in the spleen. In adding, with a important reduction in SA-beta Gal-positive area of aorta from AAV-LAV treated mice.

About energy metabolism, NAD+ can, directly and indirectly, influence many critical processes for maintaining tissue homeostasis and for healthy aging including DNA repair, chromatin remodeling, and mainly cellular senescence and immune cell functions[2,6]. As consequence, the decline in NAD+ levels accompanying

chronological aging in both humans and rodents, is one of the major culprits for the development of frailty and age-related metabolic and health decline [2].

This data support, at the functional level, the hypothesis the reduction of senescence associated inflammation ensured sustained NAD+ levels in the plasma of AAV-LAV-BPIFB4 old mice by preventing the NADase CD38 increase Ly6Chigh pro-inflammatory monocytes of the spleen and bone marrow. For the above-mentioned mechanisms, NAD+ boosting through the inhibition of CD38 is becoming a potential therapeutic strategy to improve the quality of life of aged individuals.

Chapter III – The Longevity-Associated Variant of BPIFB4 Reduces Senescence in Glioma Cells Favoring Chemotherapy Efficacy

Puca AA, Lopardo V, **Montella F**, Di Pietro P, Cesselli D, Rolle IG, Bulfoni M, Di Sarno V, Iaconetta G, Campiglia P, Vecchione C, Beltrami AP, Ciaglia E. *The Longevity-Associated Variant of BPIFB4 Reduces Senescence in Glioma Cells and in Patients' Lymphocytes Favoring Chemotherapy Efficacy.* **Cells. 2022 Jan** 15;11(2):294. doi: 10.3390/cells11020294. PMID: 35053408; PMCID: PMC8774353.

Introduction

A variety of malignant brain tumors can be classified as glioblastoma (abbreviated as GBM due to its heterogeneity). A combination of temozolomide (TMZ)-based therapy in addition to surgical resection and radiotherapy represents the standard of care for GBM patients. This established treatment approach dramatically declines since the recurrence rate is more than 90% [(1)]. Studies show that senescence plays an important role in oncogenesis and cancer aggression because senescent tumor cells release factors that are mitogenic, antiapoptotic, and angiogenesis-promoting [(2)]. This scenario (i.e., cellular senescence) has been observed in patients with glioblastoma after receiving TMZ and radiotherapy after surgery[(3)]. As a result, cancer senescent cells form heterochromatin foci associated with senescence. [(4)], They produce a spectrum of pro-inflammatory chemokines and cytokines (referred to as senescence-associated secretory phenotype, or SASP) [(5)]. This suggests that glioblastoma becomes profoundly resistant to temozolomide, triggering DNA repair mechanisms, activating multidrug resistance mechanisms, and evading immune surveillance[(6)]. In LLIs, LAV-BPIFB4 regulates the immune system's remodeling and adaptation, as well as the recovery of the inflammatory balance. As a result of LAV-BPIFB4, macrophages adopt a pro-resolving M2-like polarization state (in both microglia and atherosclerotic plaques) which improves inflammatory balance cytokine production[(7)].

On these assumptions, it was firstly indagated the function of LAV-BPIFB4 in modeling the senescence phenotype and microenvironment in an in vitro model of glioblastoma (i.e., U87-MG cells), and thus was investigated its effect in a treatment with TMZ .

Results

when it was exposed U87-MG to ETP for 5 days, it was found that the chemotherapeutic agent significantly increased the rate of U87-MG senescence-associated β-galactosidase (SA-β-gal)-positive cells, a surrogate marker of senescence, as detected by flow cytometry analysis (Fig 3.1A). Of note, when U87-MG cells were treated with recombinant LAV-BPIFB4 during the last 48 h after ETP exposure, SA-β-gal-positive cell populations significantly decreased (Fig 3.1B). Taken together, these first results indicate that LAV-BPIFB4 treatment might be able to blunt, in a specific manner, the senescence degree in GBM cells. As senescent cells may express the senescence-associated secretory phenotype (SASP) to induce and maintain the senescence phenotype in normal surrounding cells to properly burst tumor progression, it was moved to test the senotherapeutic effect of LAV-BPIFB4 on the secretion of main SASP factors which included cytokines (IL-6, IL-8 and IL-1β) and other factors such as monocyte chemotactic protein 1 (MCP1). To this end it was examined the protein levels of SASP in senescent GBM cells and in non-senescent counterpart for comparison by using multiplex ELISA. The results showed that the MCP1, IL-1β, IL-6, and IL-8 levels increased in ETP-treated U87-MG cells compared to non-senescent counterpart. The co-treatment with LAV-BPIFB4 for the last 48 h decreased all SASP factors by reaching statistical significance for IL-6 and IL-8 levels (Fig 3.1 D). No effects were reported for LAV- BPIFB4 on basal cyto-chemokine secretion from non-senescent cells (Fig 3.1 D). Collectively, these results suggest that LAV-BPIFB4 mitigates SASP induction triggered by ETP in GBM cells.

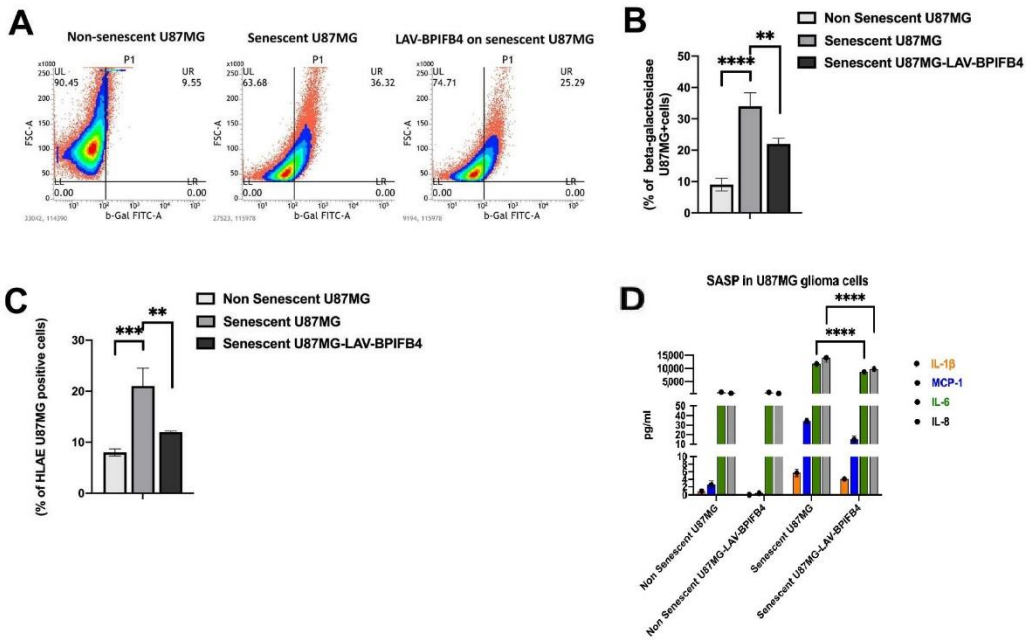

Figure 3.1 Senescence induction on U87MG cell line and LAV-BPIFB4 effects

a way to resist chemotherapy is through multi-drug-resistant P-glycoprotein (Pgp) upregulation, which acts both as a drug efflux pump and as an inhibitor of apoptosis [(9)], it was speculated that ETP-treated U87-MG cells may show high surface levels of MDR after the acquisition of drug-induced senescence phenotype. A FACS analysis was performed to assay the levels of MDR protein on the surface of U87-MG basal and ETP-treated senescent cells. The results showed that senescent U87-MG cells treated with ETP expressed a higher level of MDR than parental U87-MG cells (Fig 3.2A,B). Of interest, the co-treatment of ETP-treated senescent U87-MG cells with LAV-BPIFB4 significantly reduced the percentage of MDR positive cells (Fig 3.2A,B) . As it was herein showed that LAV-BPIFB4 blunts the degree of the senescence of cancer cells, it was speculated that LAV-BPIFB4-treated U87-MG cells may also show high sensitivity to TMZ, the first-choice chemotherapeutic agent in GBM. To test the hypothesis, first it was proved the ability of LAV-BPIFB4 to interfere with the TMZ-induced senescence. Indeed, when it was exposed U87-MG to TMZ for 24 h and 5 additional days resting, it was found a slight increase in

senescence-associated β-galactosidase (SA-β-gal) positive cells (Fig 3.2C, histograms) characterized by a higher level of p21 and p16 senescence-related markers (Fig 3.2C, WB analysis). Of note, when U87-MG cells were exposed to LAV-BPIFB4 during the last 48 h after TMZ treatment, the population of SA-β-gal-positive cells decreased. Likewise, LAV-BPIFB4 treatment induced a significative reduction of the cell cycle regulator p16 and p21, known to be essential for maintenance of the senescent cell cycle arrest. As expected, the senotherapeutic effect of the LAV-BPIFB4 was also supported by the reduced HLA-E expression (Fig 3.2E,F). Thus, it was moved to analyze the effects of combinations of TMZ and LAV-BPIFB4 in U87-MG cells in a proliferation assay. For TMZ, the fixed concentration of 100 μM was chosen. At this concentration (100 μM), the percentage of proliferating cells after 96 h was about 58 ± 3.1%. Interestingly, the co-treatment with lower doses of LAV-BPIFB4 (from 36 to 45 ng/mL) was more effective than TMZ alone in reducing proliferation of glioma cells (Fig 3.2D). Together, these findings provide new insights on the potential role of LAV-BPIFB4 in inhibiting the effects of resistance to therapy. The reduction of the senescence burden well correlated with the downregulation of HLA-E expression, which is commonly associated to the persistence of the senescent state[8]. From a mechanistic point of view, LAVBPIFB4 by reducing senescence might restore the ability of U87-MG cells to reenter the cell cycle with the consequent strengthening of TMZ-induced toxicity. This was suggested by the significant enhancement of apoptosis (both at early and late events) when TMZ-treated U87-MG cells were also exposed to LAV-BPIFB4 compared to TMZ-treated cells in which senescence and TMZ-resistance was shown (Fig 3.2G,H).

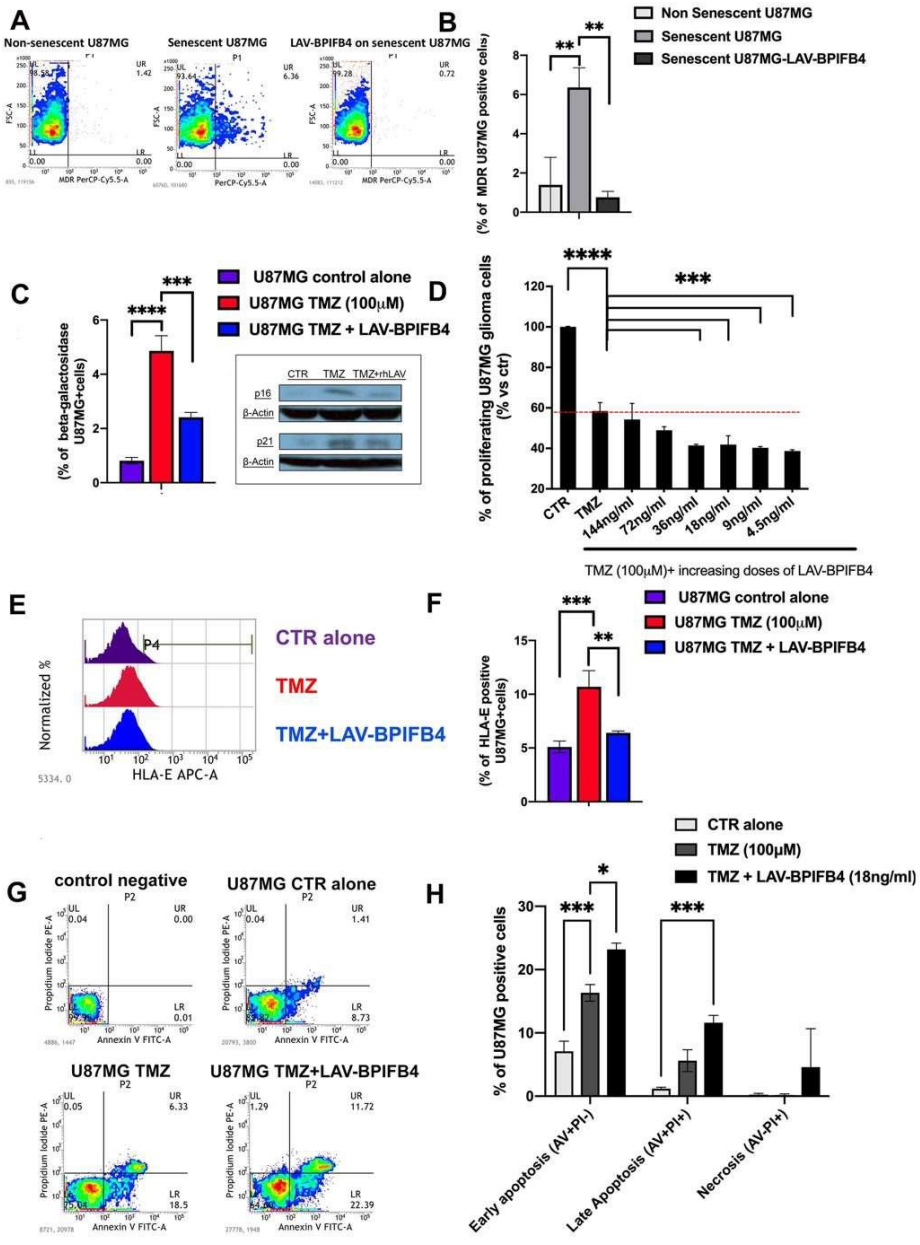

Figure 3.2 LAV-BPIFB4 effects on TMZ treated senescence cell

Methods

Cell Culture and Treatment

The U87-MG cells were cultured in EMEM (Gibco®, Thermo Fisher Scientific, Waltham, MA, USA) supplemented with 10% heat-inactivated FBS (Gibco®, Thermo Fisher Scientific, Waltham, MA, USA), 1% L-glutamine (Aurogene, Rome, Italy), 1% antibiotic mixture (Aurogene, Rome, Italy), 1% sodium pyruvate (Aurogene, Rome, Italy), and 1% non-essential amino acids (MEM NEAA, Gibco®, Thermo Fisher Scientific, Waltham, MA, USA). All cell cultures were maintained at 37 ◦C in a humidified 5% CO2 atmosphere. The U87-MG cell line was treated with temozolomide (Sigma–Aldrich, Darmstadt, Germany) at 100 µM for 96 h in the presence or absence of recombinant LAV-BPIFB4 protein at 18 ng/mL. Additionally, in order to evaluate the effect of LAV-BPIFB4 on temozolomide-induced senescence and apoptosis, U87-MG cells were pre-treated with temozolomide (100 µM) for 24 h, the medium was discarded, and fresh medium was added for an additional 5 days in the presence or absence of LAV-BPIFB4 (18 ng/mL) for the last 48 h. Similarly, U87-MG cells were also treated with etoposide (6 µM) for 24 h. After 24 h, the medium was discarded, and fresh medium was added for an additional 5 days in the presence or absence of LAV-BPIFB4 (18 ng/mL) for the last 48 h.

Senescence Induction and Detection

Glioblastoma cells (U87-MG) were treated with etoposide (6 µM) to induce senescence. After 24 h from treatment, the medium containing etoposide was removed, fresh medium was added, and the cells were incubated at 37◦C for another 5 days without further changes of medium culture. A cellular senescence detection kit, SPiDER-ßGal (Dojindo Laboratories, Rockville, MD, USA), was used following the producer's protocol for FACS analysis to verify the senescence in the cells.

Cytofluorimetric Analysis

The U87-MG cells were stained with mAb against human MDR PerCP Cy5.5 (BioLegend, San Diego, CA, USA). After 30 min incubation at 4 ◦C in the dark, cells were washed, centrifuged, and resuspended in staining buffer for the FACS analysis. For each test, cells were analyzed using a FACSVerse flow cytometer (BD Biosciences, Swindon, UK). The U87-MG cells (treated as mentioned above) were also stained for Sa-β-galactosidase and incubated for 15 min at 37 ◦C in the dark without washing before FACS analysis.

Cytokine Detection

IL-8, IL-6, IL-1β, and MCP-1 levels in the conditioned media of senescent U87-MG cells were determined using a beads-based multiplex ELISA (LEGENDplexTM, BioLegend, San Diego, CA, USA). Medium was incubated for 2 h with the beads and for 1 h with the detection antibodies, followed by 30 min incubation with SA-PE. After washing, the beads were resuspended in washing buffer and acquired using a FACSVerse flow cytometer (BD Biosciences, Swindon, UK). Data were analyzed with the LEGENDplex Data Analysis Software.

Proliferation Assay

U87-MG cell proliferation was evaluated by measuring BrdU incorporation into DNA (BrdU colorimetric assay kit; Roche Applied Science, South San Francisco, CA, USA) following treatment with temozolomide (100 µM) combined with increasing doses of LAVBPIFB4 (0–144 ng/mL) for 96 h or following treatment with LAV-BPIFB4 at 18 ng/mL without temozolomide. Newly synthesized BrdU-DNA was determined on an ELISA plate reader (Thermo Scientific, Waltham, MA, USA) at 450 nm. All experiments were performed in triplicate, and the relative cell growth was expressed as a percentage of the untreated control cells (set to 100%) to allow for an unwanted source of variation.

Cytotoxicity Assay

The Cell Counting Kit-8 (CCK-8 Cat. CK04, Dojindo Laboratories, Rockville, MD, USA) assay was performed on U87-MG cells after treatment with LAV-BPIFB4 (18 ng/mL) for 48–72–96 h. CCK-8 solution (10 µL) was added to the U87-MG cell suspension incubated for 1–4 h in a humidified incubator. Absorbance was detected at a wavelength of 450 nm. Cells 2022, 11, 294 5 of 15

Apoptosis Assay

Annexin V FITC Apoptosis Detection Kit (Cat. AD10, Dojindo Laboratories, Rockville, MD, USA) was employed to evaluate U87-MG cell apoptosis after treatment with temozolomide (100 µM) in the presence or absence of LAV-BPIFB4 (18 ng/mL). Then, 2.5 µL of Annexin V FITC Conjugate and 2.5 µL of propidium Iodide PE Solution were added to 50 µL of the cell suspension (50,000 cells/mL). After incubation for 15 min at room temperature with light protection, 200 µL of Annexin V Binding Solution was added for FACS analysis.

Western Blotting

Abs: Ab anti-p16 (BioLegend #675602, mouse mAb 1:1000, San Diego, CA, USA), Ab anti-p21 (Santa Cruz Sc6246, mouse mAb 1:1000, Santa Cruz, CA, USA) Ab anti-β-actin (Abcam #49900, mouse mAb 1: 50,000, Cambridge, UK). Immunodetection of specific proteins was carried out with horseradish peroxidase-conjugated donkey anti-mouse IgG (Bio-Rad, California, USA), using the enhanced chemiluminescence (ECL) system (Thermo Fisher Scientific, Waltham, USA) according to the manufacturer's instructions and then exposed to X-ray films (Thermo Fisher Scientific, Waltham, USA). Western blot data were analyzed using Photoshop software to determine the optical density (OD) of the bands. The OD readings of phosphorylated proteins were expressed as a ratio relative to the total protein and β-actin.

Statistical Analysis

Statistical analysis was performed for all of the experiments using GraphPad Prism 6.0 software for Windows (GraphPad software, San Diego, CA, USA). For each type of assay or phenotypic analysis, data obtained from multiple experiments were calculated as the mean ± SD and analyzed for statistical significance using ANOVA followed by Tukey's correction for multiple comparisons.

Discussion

It was disclosed a new anti-senescence effect of LAV-BPIFB4 useful for GBM tumor control. Indeed, LAV-BPIFB4 treatment downregulates senescence both in cancer cells in vitro and in T lymphocytes from GBM patients, a key event which may support a dual activity of LAV-BPIFB4 in the cancer microenvironment. It was demonstrated that LAVBPIFB4 can specifically counterbalance the therapy-induced senescence (Fig 3.1 and 3.2), a state which is responsible for a chronic secretory phenotype that is generally considered pro-tumorigenic and promigratory, especially in GBM residual disease. It was reported that LAV-BPIFB4 treatment reduces selectively IL-6 and IL-8 (Fig 3.1), from U87-MG cells, two cytokines known to maintain glioma stemness and create a supportive niche for GBM recurrence. Consequently, LAV-BPIFB4 downregulated the surface of the non-classical MHC molecule HLA-E on the senescent U87-MG cells (Fig 3.2 E-F), recently reported to be induced by SASP-related pro-inflammatory cytokines reducing GBM immunogenicity. As regards the cancer cell compartment, it was tested the LAV-BPIFB4 effect against the senescence response upon both ETP or TMZ treatment. The downregulation of MDR level by LAV-BPIFB4 on the surface of ETP treated senescent cells (Fig 3.2 A-B) may be a general mechanism valid also for explaining the better response to TMZ. In fact, it has been shown that inhibition and control of the MDR complex correlate with an increased sensitivity of GBM to temozolomide. Furthermore, in TMZ-exposed glioma cells, the pre-treatment with LAV-BPIFB4 may restore the ability of these cells to reenter the cell cycle and may cause the TMZ-induced toxicity, as suggested by the higher apoptotic rate induced by LAV-BPIFB4 co-treatment (Fig 3.2 G,H).

In summary, even though the related mechanisms of such effects need to be deeply dissected, in the future, treatment with LAV-BPIFB4 as well as other senotherapeutics, might be a valuable strategy to restore therapy-sensitivity and a proper immune surveillance.

Chapter IV – LAV-BPIFB4 reduces progression in a mouse model of Huntington's disease by a CXCR4 modulation

Di Pardo A, Ciaglia E, Cattaneo M, Maciag A, **Montella F**, Lopardo V, Ferrario A, Villa F, Madonna M, Amico E, Carrizzo A, Damato A, Pepe G, Marracino F, Auricchio A, Vecchione C, Maglione V, Puca AA. *The longevity-associated variant of BPIFB4 improves a CXCR4-mediated striatum-microglia crosstalk preventing disease progression in a mouse model of Huntington's disease*. **Cell Death Dis. 2020 Jul** 18;11(7):546. doi: 10.1038/s41419-020-02754-w. PMID: 32683420; PMCID: PMC7368858.

Introduction

Huntington's disease (HD) is an autosomal dominant inherited neurodegenerative disorder. This disease is caused by a CAG repeat expansion within the HTT gene, which encodes huntingtin protein (Htt), which, when mutated (mHtt), exerts a variety of undesirable toxic effects on neurons and nonneuronal cells. Specifically, CAG repeat length of up to 35 repeats generally does not result in the onset of HD[1,2] . However, individuals with repeat numbers from 36 up should be viewed at as at risk of developing HD. CAG repeat lengths of >40 are associated with a definite onset of HD within a normal lifespan. Microglia play a crucial role in disease progression based on our knowledge of neuroinflammation in HD. To maintain the brain's homeostasis, these myeloid-derived immune cells oscillate between a surveilling and activated state. As a result of the local environment and recent exposure to stimuli, microglia exhibit a dynamic, context-dependent expression phenotype[3]. It has been proposed that an imbalance between pro- and anti-inflammatory state of microglia might contribute to bipolar disorder, amyotrophic lateral sclerosis, multiple sclerosis (MS), and Rett syndrome[4]. Several human and animal studies have reported that a M1/M2 microglia imbalance is beneficial or detrimental depending on the stage of the disease[5]. In fact, microglia, astrocytes, circulating cytokines, macrophage infiltration, as well as changes in

gene transcription associated with inflammation have been observed in HD[6]. In this view, the LAV-BPIFB4 pleiotropic ability, both in immune compartment and cellular homeostasis, challenged to investigate its potential role as a new promising immunoregulatory agent in HD. In the present study, it was shed light on the LAV-BPIFB4 therapeutic potential by gene transfer adopting either a cellular model of striatal-derived cell lines and their crosstalk with microglia.

Results

STHdh striatal cells represent a widely used cell culture model for studying cellular aspects of HD pathology. In the present study, specifically, it was used STHdh Q7/7 and STHdh Q111/111 cell lines (which it was refer to as Q7 and Q111, respectively, in figures) derived from a knock-in mouse model of HD and endogenously expressing fulllength Htt with either short (Q7) or long (Q111) polyglutamine (polyQ) repeats[7]. A putative mechanism for toxicity of long polyQ proteins is through a dysregulated proteasome activity. This is a multicatalytic protein complex that regulates cellular protein turnover, as well as the cell cycle, signal transduction, and survival of the cell[8]. Thus, to corroborate the adequacy of the cell model used to describe the results, it was started to test the response to proteasome blocking in term both of cell cycle arrest (Fig. 4.1a) and cytotoxicity (Fig. 4.1b) on STHdh Q7/ Q7 and STHdh Q111/Q111 cell lines treated or not with the proteasome inhibitor MG-132 (5 μM). As reported in Fig. 4.1a, after 24-h treatment STHdh Q7/Q7 had a higher percentage of BrdU+ proliferating cells compared to STHdh Q111/Q111 cells. The observed differences in proliferative rate were in line with the reduced amount of STHdh Q111/Q111 viable cells compared to STHdh Q7/Q7 cells, explainable with a better ability of the latter to cope with the conditions of proteotoxic stress (Fig. 4.1b). As a result of the altered response of two cell lines, it was examined the differential protein levels of BPIFB4. Western blot analysis showed a significant downregulation of the BPIFB4 immunoreactivity in mutant STHdh Q111/Q111 cells compared to wild-type STHdh Q7/Q7 (Fig. 4.1c, right histogram). In agreement, enzyme-linked

immunosorbent assay (ELISA) analysis showed a decreased BPIFB4 secretion in the STHdh Q111/Q111 compared to the nonmutant striatal cells (Fig. 4.1d).

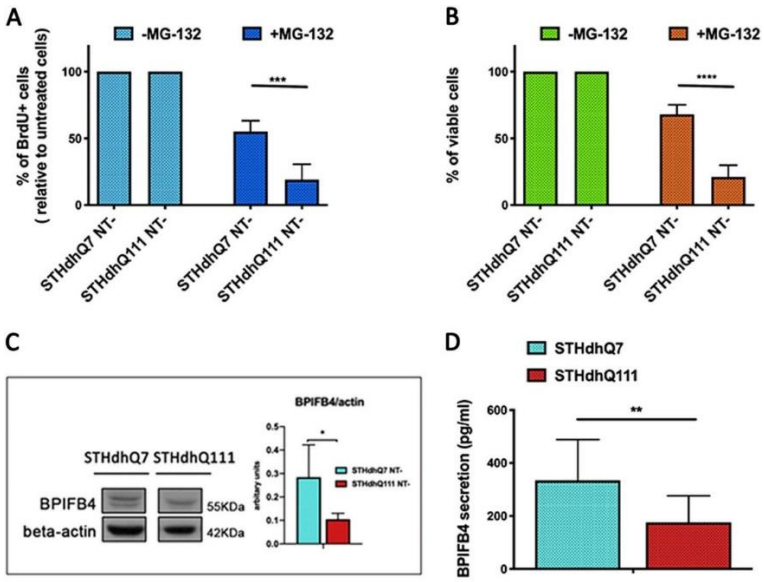

Figure 4.1 Different features in STHdh Q7/7 and STHdh Q111/111 cell line concerning the sensitivity to stress induced by proteasome blocking and the BPIFB4 expression profile.

Considering that BPIFB4 cellular levels are significantly reduced in STHdh Q111/111, it was examined whether overexpression of human BPIFB4 isoforms can rescue the defective response in STHdh Q111/111. To this end, it was examined the secretory profile and changes both in the proliferation and the cell viability of the mutant STHdh Q111/111 in response to lentivirus-mediated overexpression of human BPIFB4 isoforms (both WT- and LAV-BPIFB4). At functional level, a recovery of the BPIFB4 secretory profile (Fig. 4.2a) and a better response to the inhibition of the proteasome (Fig. 4.2b, c) were observed following infection with LAV-BPIFB4. Indeed, the percentage of STHdh Q111/111 viable and proliferating cells under MG-132-induced stress was statistically higher in striatal cells infected with LAV-BPIFB4 than either untreated or empty vector-infected striatal cells. Most importantly, the restoration of a defective proliferation

(Fig. 4.2b) and the survival recovery (Fig. 4.2c) paired with the statistically significant increase in the BPIFB4 secretory profile that shows the highest BPIFB4 protein levels by STHdh Q111/111 infected with LAV-BPIFB4 (Fig. 4.2a). The achieved results supported the protective effects of LAV-BPIFB4 and BPIFB4 secretion against insults induced by mHtt in STHdh Q111/111, such as impaired heat shock response and loss of proteostasis described in previous reports[9], processes already showed to be activated by BPIFB4 overexpression.

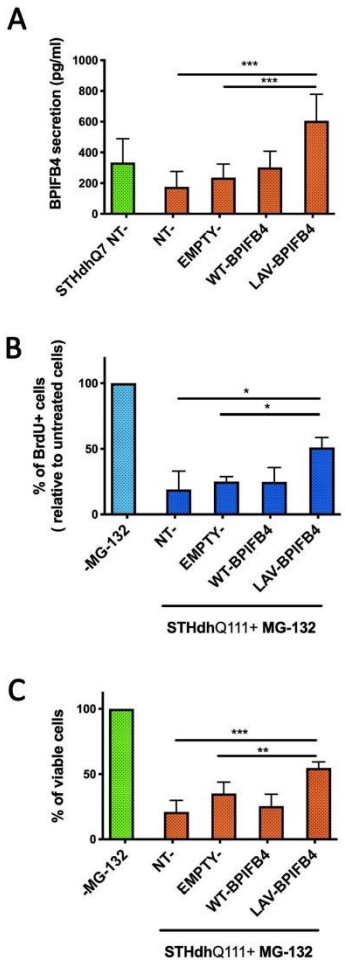

Figure 4.2 Effects of BPIFB4 infection on the defective proliferation and the viability and the BPIFB4 protein secretion in STHdh Q111/111 cell line

As recently reported, LAV-BPIFB4-treated mice showed increased stromal cell-derived factor-1 (SDF-1) levels in peripheral blood and myocardium. SDF1 upregulation was instrumental to LAV-BPIFB4-induced benefit as both haemodynamic and structural improvements were inhibited by an orally active antagonist of the CXCR4 receptor. Beyond its chemotactic activity, SDF-1/CXCR4 axis enhances the immunomodulation. of the secreting cells in alleviating the inflammatory processes. It was previously demonstrated that BPIFB4 polarizes macrophage M2 via a mechanism mediated by CXCR4, so it was decided to examine SDF-1 chemokine secretion in an experimental model after BPIFB4 infection. Interestingly, ELISA analysis confirmed that STHdh Q111/111 infected with LAV-, but not WT-BPIFB4, secreted higher level of SDF-1 compared to the untreated striatal cells (Fig. 4.3A). HM-SV0 microglial cells were next cultured in vitro in STHdh medium (CM) to determine whether soluble factors released by infected striatal cells could influence M2-polarization. The panels b and c in Fig. 4.3 showed a cytofluorimetric analysis of CD163 surface marker on HMSV40 microglia. Interestingly, normal cells (STHdh Q7/7) induced the cell surface upregulation of CD163 proresolving marker on HM-SV40. While this ability was lost in mutant STHdh Q111/111 cells, where a significant increase in the percentage of CD163+ cells and IL-10 release (Fig. 4.3D) was observed after 48-h treatment with CM from LAV-BPIFB4-infected STHdh Q111/111. The CXCR4-dependent mechanism was confirmed by the decreased CD163 amount and IL-10 secretion after treating HM-SV40 microglial cells with the CXCR4 antagonist AMD3100 (20 μM).

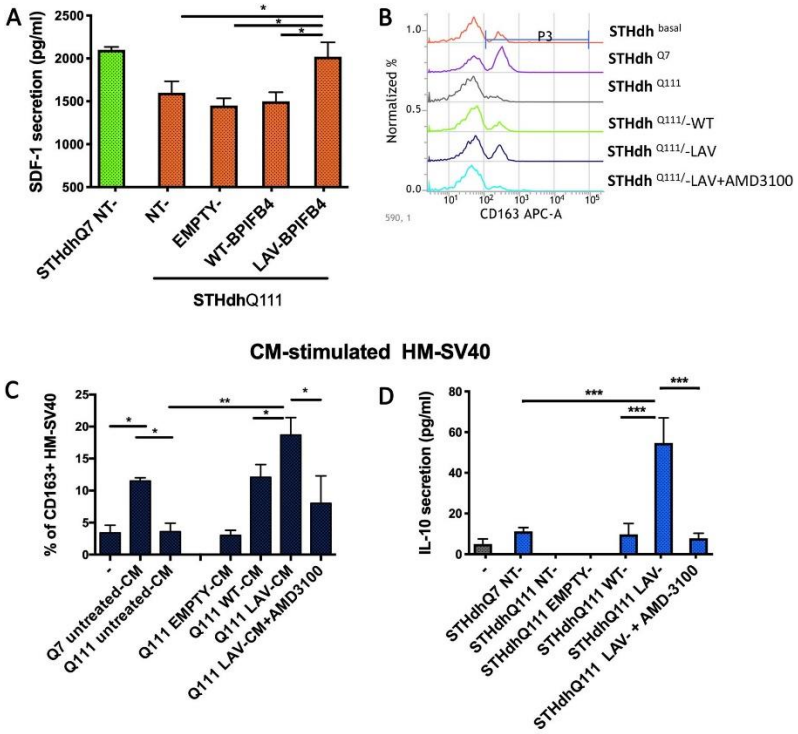

Figure 4.3 Analysis of anti-inflammatory and M2-polarizing action of CM from LAV-BPIFB4-infected striatal cells.

Methods

Cell lines, culture condition, lentiviral infection, and conditioned media Immortalized striatal cells (STHdh) derived from a knock-in transgenic mouse containing homozygous Htt loci with a humanized Exon1 with either short (STHdh Q7/7) or long polyQ repeats (STHdh Q111/111) were grown at 33 °C in 10% FBS in DMEM. Properly authenticated cells were purchased from the Coriell Cell Repositories (Coriell Institute for Medical Research, Camden, NJ, USA). STHdh Q111/111 cells were infected with empty lentiviral vector or particles encoding either WT- or LAV-BPIFB4. After 72 h, cells were selected with 2 µg/ml puromycin for 48 h. BPIFB4 expression was tested by real-time PCR and WB. In order to obtain the CM, DMEM-FCS medium was discarded, the cells were washed three times and subsequently cultured for 72 h. After that the media from both STHdh Q7/7 and STHdh Q111/111 were collected and stored in aliquots frozen. This medium was

considered CM and used at 20% for subsequent treatments. Properly authenticated cells HM-SV40 (Cat. No.: T0251) cell lines were purchased from Applied Biological Materials Inc (Richmond, QC, Canada). HM-SV40 were grown in Prigrow III media containing 10% FCS and antibiotics in Applied Biological Materials Inc (Richmond, QC, Canada) in Corning T75 coated flask with collagen I at 0.1 mg/mL (Cat. No.: A10483-01—Gibco Life Technologies Corporation, Grand Island, NY, USA) concentration. Briefly, flasks were treated with collagen 0.1 mg/mL in PBS with calcium and magnesium (Cat. No.: D1283—Sigma-Aldrich, St.Louis, MO, USA) for 1 h at 37 °C; after that, two washes in PBS with calcium and magnesium were needed and flasks were used to seed the cells. Cells were splitted at the 80% of the confluence.

Cell viability assays

Cell viability was determined using commercially available kit (Cell Counting kit-8, Dojindo) following the provider's instructions. In the last 1–4 h of treatment 20 μL of CCK-8 solution was added to 200 μL of cell suspension seeded in a 96-well plate and incubated at 37 °C. Absorbance at 450 nm was measured using a microplate reader.

Determination of STHdh Q7/7 and STHdh Q111/111 cell proliferation

STHdh Q7/7 or STHdh Q111/111 cells (6 × 103/well) were cultured for 24 h into 96-well plates before addition of MG-132 at the indicated concentration and cultured for additional 24 h at 37 °C. Cell proliferation was evaluated by measuring BrdU incorporation into DNA (BrdU colorimetric assay kit; Roche Applied Science, South San Francisco, CA, USA). Newly synthesized BrdU-DNA was determined by an ELISA plate reader (ThermoScientific) at 450 nm. All experiments were performed in triplicate, and the relative cell growth was expressed as a percentage in comparison with the untreated control cells (100%).

Western blotting

Western blot analysis was performed following standard procedures. 30 μg of protein was separated electrophoretically using 10% SDSpolyacrylamide gel (Bio-Rad). Proteins were transferred on 0.2 μm Trans-Blot® Turbo™ Mini Nitrocellulose membrane (Bio-Rad) using a Trans-Blot® Turbo™ Transfer System (Bio-Rad #1704150). Membrane was blocked with 5% milk (Bio-Rad, Richmond, CA, USA) in TBS containing 0.1% Tween-20 (TBST) at room temperature for 1 h and probed overnight at 4 °C with the primary antibodies: mouse anti-β-actin (1:30,000; Ab49900, Abcam) and rabbit anti-BPIFB4 (1:1000, custom made). Afterwards, membrane was incubated at room temperature for 1 h with the respective secondary antibodies. The immunoblots were visualized by using the enhanced chemiluminescence method using Amersham ECL.

Enzyme-linked immunosorbent assay

BPIFB4 levels in STHdh-conditioned media were determined using Human Long palate, lung, and nasal epithelium carcinoma-associated protein 4 (C20orf186) ELISA kit (Cusabio CSBYP003694HU) following the manufacturer's protocol. STHdh-conditioned media SDF-1 levels were determined using DuoSet® ELISA Development Systems (R&D systems) following the manufacturer's protocol. STHdh-conditioned media IL-10 levels were determined using a beads-based multiplex ELISA (LEGENDplex, Biolegend, USA). Conditioned media were incubated for 2 h with the beads and detection antibodies, followed by 30 min incubation with SA-PE. After washing, beads were resuspended in washing buffer and acquired using a FACS VERSE flow cytometer (BD Biosciences). Data were analyzed with the LEGENDplex Data Analysis Software.

Antibodies and flow cytometry

Cell suspensions were stained with mAb against human CD163 (REA812; Miltenyi Biotec GmbH; 1:50). After 20 min incubation at 4 °C in the dark, cells were washed, centrifugated, and resuspended in staining buffer for the FACS analysis. For each test, cells were analyzed using FACS Verse Flow Cytometer (BD Biosciences).

Discussion

Both in aged brain and in HD, a sustained inflammation often compromises neuronal viability and correlates with the degree of neurodegeneration. The biological role of immune responses might disclose a rapidly emerging field of study for therapeutic intervention. The ability of BPIFB4 to regulate cellular homeostasis and fine-tune immune responses lead to investigate its role in neurodegenerative disorders. Here, it was reported for the first time the different expression levels of BPIFB4 in normal Q7/7 versus mutant Q111/111 striatal cells (Fig. 4.1c, d). Furthermore, it was presented previously unrecognized effects of the LAV-variant in restoring the defective proliferation (Fig. 4.2b) and the survival response of cells exposed to stress (Fig. 4.2c), probably in an auto-paracrine manner, as the sustained BPIFB4 secretory profile (Fig. 4.2d) seems to be instrumental to preserve STHdh Q111/111 cellular proteostasis upon MG-132 insult. From a mechanistic point of view, using CXCR4 inhibitor, it was demonstrated that SDF-1/CXCR4 axis plays a critical role in LAV-BPIFB4 beneficial effects in vitro (Fig. 4.3). Even though the mechanism by which LAV-BPIFB4 induces SDF-1 expression is still unknown, the relevance covered by the SDF-1 in myeloid cell differentiation, tissue repair and stem cell mobilization, might in part explain the beneficial effect achieved by LAV-BPIFB4 therapy in the context of HD. Collectively, this evidence corroborates the specificity of the favorable connection between LAV-, but not WT-BPIFB4, and SFD-1/CXCR4 signaling pathway in HD. In near future, given the dual action both on striatum and immune surveillance, it was propose that the gene transfer or alternatively the usage of a human recombinant protein of LAV-BPIFB4 in presymptomatic HD carriers may represent a promising strategy to improve HD symptoms or delay its onset.

Platelets express the BPIFB4 protein and contribute to the functional effects of the LAV-BPIFB4 polymorphic variant

Introduction

Platelets are figurative elements of the blood, anucleate, with the function of mediating the coagulation process, capable of closing a wound, and therefore haemostasis. They develop by fragmentation from marrow extraction precursors called megakaryocytes. They have a short half-life, at the end of which they are eliminated in the spleen[1]. In addition to regulating haemostasis, platelets can influence the inflammatory response, in particular the innate immune processes. Their pro-inflammatory effects on circulating leukocytes are reported in the literature, attracting immune cells to the site of damage and activating them in response to the release of cytokines[2]. The different proteins and molecules necessary for the post-inflammatory healing and repair process are secreted by three types of granules (alpha, delta and lambda) located within the platelets. The content of α-granules is very heterogeneous with regards to their function and include proteins involved in coagulation, inflammation, cell growth, adhesion and host defense. There are both typical cytokines of inflammatory processes and those involved in the processes of repair and shutdown of inflammation[3,4]. The delta granules contain factors that stimulate coagulation processes such as calcium, magnesium, ADP and bioactive amines such as serotonin and histamine. Lambda granules are mainly responsible for the reabsorption of debris or other circulating proteins (such as the same cytokines and growth factors) for subsequent enzymatic degradation.

Several studies have shown that platelets display also antimicrobial effects against bacteria, viruses, fungi, and protozoa[5,6]. Platelet-bacteria interactions are complex due to a variety of platelet receptors involved in recognizing bacteria. Several bacterial receptors are found on platelets, including complement receptors, Fc-RIIa,

TLRs, GPIIb-IIIa, and GPIb[7]. Upon contact with certain bacteria, platelets can become activated, aggregate, and degranulate. Over 300 secretory products are released by activated platelets, including antimicrobial products (collectively known as platelet microbicidal proteins (PMPs))[8]. There are four family members of PMPs that are released from platelets. These include kinocidins (CXCL4, CXCL7 and CCL5), defensins (human defensin 2), thymosin, and derivatives of PMPs (thrombocidins). Recent studies have demonstrated the expression of defensin 1 in human platelets as well as the activity of this antibacterial peptide[9].

A secreted protein with a role of natural defensin and immunomodulatory properties, named BPIFB4 (bactericidal/permeability-increasing fold-containing family B, member 4) has been found in respiratory secretions, upper airways, and proximal trachea[10]. It has been also found in cardiomyocytes and endothelial cells[11], Peripheral Blood Mononuclear Cells (PBMCs)[12], and striatal-derived cell lines[13]. The abundance of BPIFB4 in the serum of Long Living Individuals associates with their ability to maintain a healthy balance between anti-inflammatory and proinflammatory mechanisms without experiencing the adverse immune system remodeling typically associated with aging[14]. Further, over the past few years, GWASs (Genome-Wide Association Studies) have been conducted on LLIs and controls in order to determine whether genetic variants may confer advantage or disadvantage when reaching extreme ages. A single-nucleotide polymorphism associated with the BPIFB4 gene known as LAV-BPIFB4 (Longevity Associated Variant) has been found to be enriched in LLIs, thus protective for human health, in three independent populations in Italy, Germany and the United States[15], with an allele frequency of 29.5% compared to 66% of the Wild Type (WT) haplotype. Since then, *LAV-BPIFB4* gene therapy demonstrated anti-atherosclerotic,[11] anti-hypertensive, pro-angiogenic,[8] and neuroprotective activities,[12] improved frailty indices,[13] rescued diabetic cardiomyopathy and delayed cardiac aging and ischemic heart dysfunctions.[14] The translational value of these studies was successful confirmed by the efficacy of the recombinant LAV-BPIFB4 protein that was equally

effective in transferring the healthy phenotype of LLIs to murine models and cultured human tissues. Indeed, atherosclerosis patients' macrophages acquired a favorable M2 anti-inflammatory phenotype following exposition to the recombinant protein[17]. At the same way, the application of rhLAV-BPIFB4 also improved endothelial-mediated vasorelaxation of human atherosclerotic vessels via increased eNOS phosphorylation (EHJ). Furthermore, as a result of pretreatment with rhLAV-BPIFB4, human CD14+ monocytes and monocyte-derived dendritic cells released less TNF-a and IL-1b, confirming the ability of this protein variant to maintain an anti-inflammatory microenvironment[16].

The protein carrier role of platelets and their influence on the immune system prompted to investigate the involvement of platelets in the immune modulatory role of the BPIFB4 protein, also considering its abundance in the circulatory system. The present work highlights that BPIFB4 harbored in MK-platelets compartment was instrumental in the LAV-BPIFB4 gene modulatory effects on both immune compartment and vascular reactivity in vivo. Finally, to understand the functional role of BPIFB4 in platelets, it was stimulated platelets with rhLAV-BPIFB4, and surprisingly described for it both an inhibitory effect on platelet-platelet aggregation *in vitro* and an antithrombotic activity *in vivo.*

The present work provides new insights into BPIFB4 role, highlighting that BPIFB4 harbored in MK-platelets compartment was instrumental in the LAV-BPIFB4 gene modulatory effects on both immune compartment and vascular reactivity in vivo. Finally, to understand the functional role of BPIFB4 in platelets, it was stimulated platelets with rhLAV-BPIFB4, and surprisingly described for it both an inhibitory effect on platelet-platelet aggregation *in vitro* and an antithrombotic activity *in vivo.*

Results – Unpublished Data

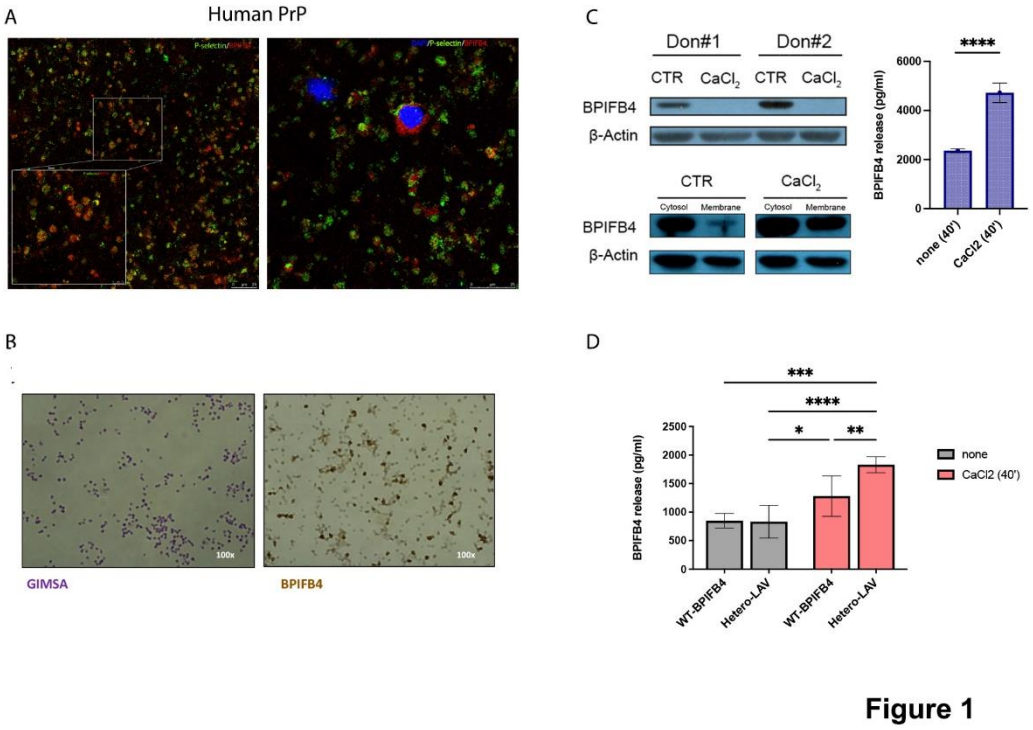

Figure 1

Figure 5.1 BPIFB4 content in human platelets

To investigate the extent and expression pattern of BPIFB4 in the platelets, it was analyzed platelets from human platelet-rich plasma properly stained with fluorescent-labelled antibodies against P-selectin, a common platelets marker, and BPIFB4 (Fig. 5.1A). P-selectin, is mostly located in the α-granule membrane of resting platelets and only found on the platelet surface after platelet activation (review plt). Double-label immunofluorescence confocal microscopy on fixed and permeabilized platelets revealed a large intracellular localization of BPIFB4. This was also consistent with the BPIFB4 immunoreactivity in thrombocytes, as reported in Fig. 5.1B. Interestingly, the BPIFB4 stain labeled punctate, vesicle-like structures distributed throughout the platelet cytoplasm, suggesting its putative release. As expected, Western Blot analysis of human PRP lysates, which indicate platelet cargo, revealed that resting human platelets contained high levels of BPIFB4; but platelets

activation with calcium chloride (CaCl2) resulted in total disappearance in BPIFB4 levels (Fig.5.1C). Conversely, in releasates representing the released secretory cargo of PRP, the level of BPIFB4 significantly increased after platelet activation (Fig. 5.1D). Moreover, genotype stratification analysis of human PRP showed that LAV-BPIFB4 carriers released higher levels of BPIFB4 after platelet activation when compared with no-carriers (Fig.5.1E).

As circulating levels of BPIFB4 were associated with protection against the onset of several disease, such atherosclerosis, severe COVID-19 and coronary artery disease (CAD), the findings that BPIFB4 haplotype led to unique protein release signature from platelets, may provide a mechanistic understanding of its functional effects.

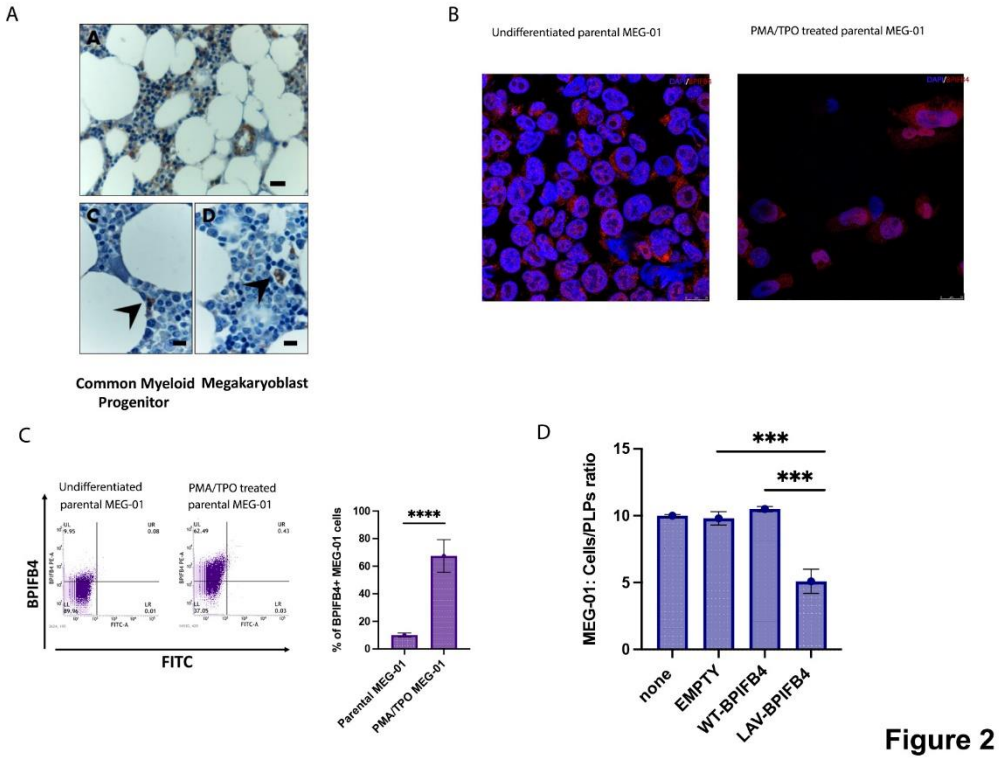

Figure 5.2 BPIFB4 expression: from myeloid progenitors to platelet release

To evaluate whether the expression of BPIFB4 previously found in platelets could also involve the upstream platelet precursors, it was explored BPIFB4 in the different megakaryopoiesis stages' cell types. Common myeloid progenitors and megakaryoblasts are the earlier platelet precursors. As shown in Fig. 5.2A, BPIFB4 positive cells in bone marrow were found to be myeloid lineage cells, considering the DAB staining. Even if the low number of positively stained common myeloid progenitors and megakaryoblasts, IHC double staining demonstrated the expression of BPIFB4 in these platelet precursors. Megakaryoblasts undergo several endomitosis steps and at the final stage give rise to granular megakaryocytes supported by multiple growth factors, as thrombopoietin. Subsequently, each mature megakaryocyte is able in releasing thousands of platelets. In order to study BPIFB4 expression in megakaryocytes, it was handled MEG-01 cells, a megakaryoblastic cell line which is a useful in vitro model for studying megakaryopoiesis and platelets' formation. Indeed, MEG-01 cells have morphological and phenotypical features resembling those of megakaryocytes, spontaneously release platelet-like particles and can be differentiated by PMA and TPO into mature megakaryocytes. As reported in Fig. 5.2B, BPIFB4 appeared slighlty expressed and mainly localized in cytoplasmic area of undifferentiated MEG-01 cells while PMA/TPO treatment of cells, leading to differentiation, resulted in both increase and transfer of BPIFB4 towards MEG-01 nuclei. As expected, flow cytometry analysis of BPIFB4 in naive and differentiated MEG-01 showed a significative increase of the percentage of BPIFB4+ MEG-01 cells upon PMA/TPO-induced differentiation of megakaryocytes (Fig. 5.2C). To deepen the biological value of BPIFB4 expression in differentiated MEG-01, it was evaluated the impact of the overexpression of human WT- and LAV-BPIFB4 isoforms in MEG-01. Interestingly, the lentivirus-mediated overexpression of human LAV-BPIFB4 isoform was able in leading differentiated megakaryocytes to release more platelets, as shown by the lessened MEG-01 cells/platelet-like particles ratio of LAV-BPIFB4 MEG-01 cells and PLPs, reported in Fig. 5.2D. Taken together these results suggest BPIFB4 emerges in multiple steps of the

megakaryopoiesis process and the longevity-associated variant might be functional to platelet release.

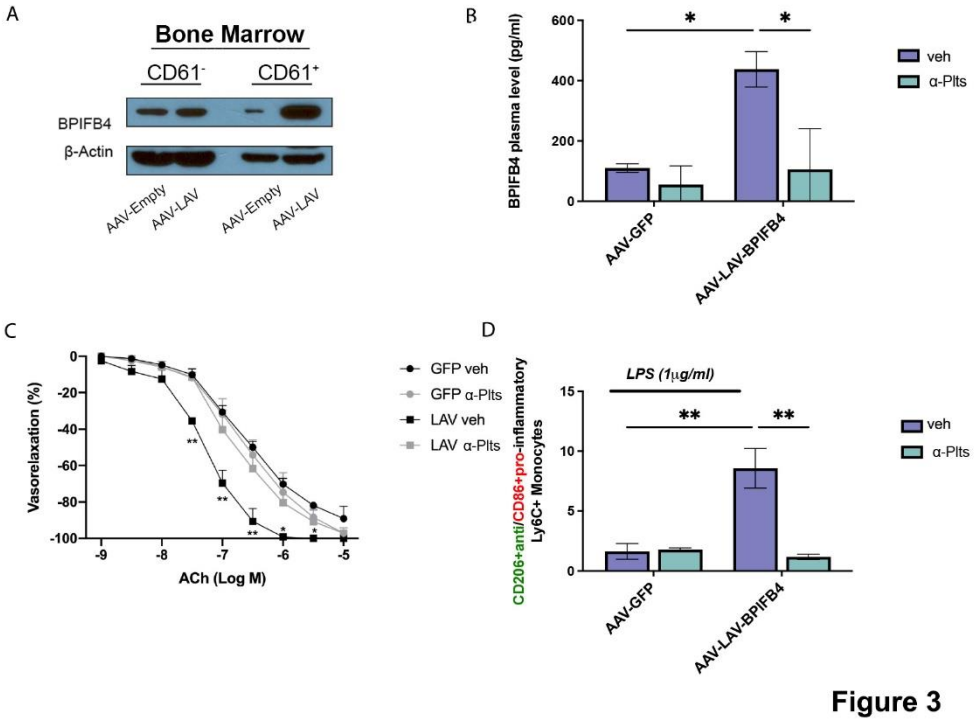

Figure 3

Figure 5.3 Platelets contribute to the pool of BPIFB4 in plasma and its effects on both vascular reactivity and monocyte inflammatory profile.

Because BPIFB4 was highly expressed in platelets, it was questioned whether BPIFB4 protein expression was coordinately increased also in megakaryocytes precursors after LAV-BPIFB4 gene transfer. First, when LAV-BPIFB4 gene was delivered using adeno-associated viral (AAV) vectors into femoral arteries of C57BL/6 (wild-type) mice, it was efficiently monitored a BPIFB4 enrichment in bone marrow niche of AAV-LAV but not AAV-EMPTY-mice in accordance with previous published results. Then, as expected, western blot analysis for total BPIFB4 on whole cell extracts from murine platelet glycoprotein IIIa (CD61+) positive cells, isolated through an immunomagnetic procedure on single-cell suspensions,

highlighted a selective enrichment of BPIFB4 in large CD61+megakaryocytes, compared to CD61- myeloid counterpart (Fig. 5.3A), confirming the immunostaining experiments previously reported (Fig. 5.2A-B). As the MK-Plts compartment are a good source of BPIFB4, then it was sought to characterize the contribution of platelets to the pool of BPIFB4 in plasma and to the proper protein functionality after AVV-LAV-BPIFB4 gene transfer in vivo. Mice were divided in two groups and treated with either α-CD42b (α-Plts) or an antibody control (veh) 4 days after AAV-LAV-BPIFB4 gene delivery. Antibody-mediated platelets depletion resulted in a >80% reduction in circulating platelets count. As expected, in platelet-competent mice, the BPIFB4 plasma levels after 4 days from treatment with AAV-LAV-BPIFB4 significantly increased compared to AAV-EMPTY. Moreover, BPIFB4 levels were significantly elevated compared to platelet-depleted mice (Fig. 3B). Furthermore, in platelet-competent mice, the monocyte CD206+anti-/CD86+pro-inflammatory Ly6C+ ratio after ex vivo LPS- stimulation was significantly elevated in AAV-LAV-BPIFB4 treatment group compared to platelet-depleted mice (Fig. 5.3C), demonstrating that platelets are function to anti-inflammatory effects of AAV-LAV-BPIFB4 gene transfer compared to control AAV-EMPTY mice group. Further, skewing to a heightened anti-inflammatory state and high plasma level of BPIFB4 in platelet-competent AAV-LAV-BPIFB4-mice was supported by an improvement of the vascular reactivity of ex vivo mesenteric arteries to Acetylcholine. In contrast, platelet depletion in mice treated with AAV-LAV-BPIFB4 completely abolished the beneficial effect of AAV-LAV-BPIFB4 (Fig. 5.4D), indicating a direct participation of platelets or BPIFB4 released from them in AAV-LAV-BPIFB4 therapeutic effects.

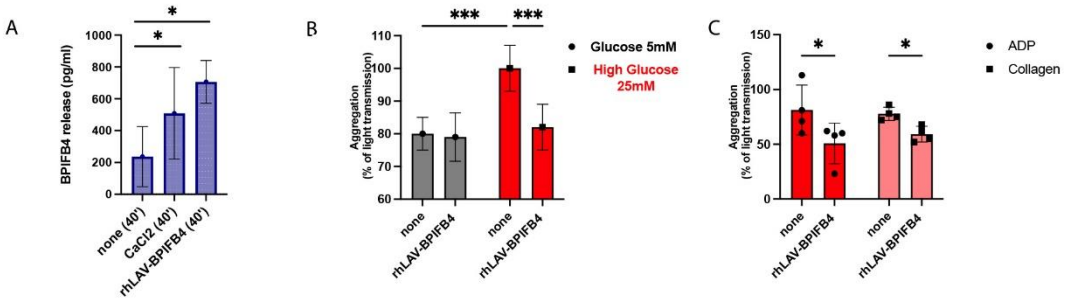

Figure 4

Figure 5.4 Effects on human platelets of recombinant LAV-BPIFB4.

As suggested by previous report, a valuable therapeutic tool able to recapitulate the association of genotypes with LAV-BPIFB4 gene effects, is the treatment with the recombinant protein rhLAV-BPIFB4. Thus, to understand the functional role of BPIFB4 harbored in platelets, it was stimulated human platelets with recombinant LAV-BPIFB4. As first, it was performed an ELISA assay to determine the entity of BPIFB4 release after treatment with 20ng/ml of recombinant LAV-BPIFB4. Compared to calcium chloride (22mM), used a positive activating stimulus, rhLAV-BPIFB4 induced a massive release of endogenous BPIFB4 after 40 minutes of treatment of washed platelets. (Fig 5.4A). Concerning protein release, since the effects of rhLAV-BPIFB4 mimicked those of calcium chloride, which is a pro-aggregating stimulus, it was tested if the recombinant protein might influence platelets activation. To analyze platelet-platelet aggregation, it was evaluated three different activating conditions. First, it was analyzed the effect of the recombinant

protein in a context of low glucose (5mM) stimulation, after that the analysis was performed with high doses of glucose (25mM), simulating a diabetic condition. Of note, rhLAV-BPIFB4 did not induce platelet aggregation, but on the contrary significantly reduced it when induced by high glucose concentrations (Fig 5.4B). Finally, in a small cohort of treatment-naive patients with type 2 diabetes, it was studied the anti-aggregating effects of rhLAV-BPIFB4 treatment after high doses of ADP (20 μM) or Collagene (0,19mg/ml), simulating a cardiovascular damage. Meanwhile ADP and Collagene agonist stimulation induced high aggregation, the co-treatment with rhLAV-BPIFB4 significantly reduced the activation capacity of patients' platelets.(Fig 5.4C).

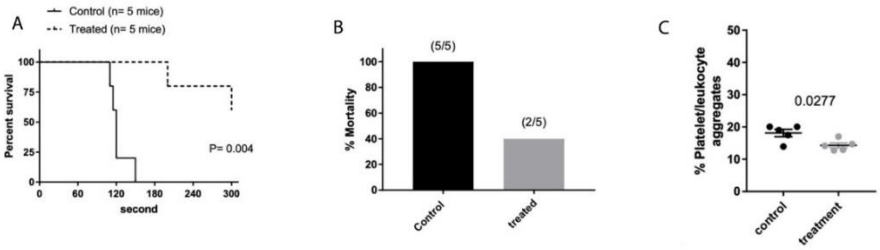

Figure 5

Figure 5.5 rhLAV-BPIFB4 displays effective anti-thrombotic activity in vivo

To gain insight into the role of LAV-BPIFB4 on platelet aggregation and its therapeutic potential in vivo, next it was assessed the rhLAV-BPIFB4 efficacy in inhibiting thrombus formation in a murine model of lethal pulmonary

thromboembolism. To this end, a collaborator from "Unit of Brain-Heart Axis: Cellular and Molecular Mechanisms, Centro Cardiologico Monzino" has was evaluated the mortality associated with an intravenous i.v. injection of collagen after administration of either PBS (control) or rhLAV-BPIFB4. Animals that were alive 5 min after the challenge were considered to be survivors. Fig. 5.5B shows that all mice (5/5) died within 3 min of i.v. administration of collagen. In contrast, the group of rhLAV-BPIFB4–treated mice showed a significant number of survivors (3 out of 5 at 3 microg/mouse of rhLAV-BPIFB4). As a result of reduced platelets' activation, lower level of circulating leukocyte-platelets aggregates (LPA) was found in rhLAV-BPIFB4-treated mice compared to control (Fig. 5.5C). Overall, an administration of rhLAV-BPIFB4 24 hours before tromboembolism induction protected from induced thromboembolism-related mortality as an effective antithrombotic agent.

Methods

Patients' Recruitment

To perform the study a cohort of N=4 naïve to treatment diabetic patients was considered. Peripheral blood samples were collected from each patient within 7 days from admission to "Giovanni di Dio e Ruggi d'Aragona" University Hospital of Salerno. Human PrP samples were also collected from 17 healthy donors and secondly divided according to genotype in etero, WT and LAV (etero: N=6; WT: N=8; LAV: N=3) according to the variant of the protein BPIFB4 owned. All participants signed an informed consent for the management of personal anamnestic data and blood samples. The study was approved by the IRCCS MultiMedica and by the internal Ethics Committee of "Giovanni di Dio e Ruggi d'Aragona" University Hospital of Salerno and was conducted in accordance with the ethical principles of the Declaration of Helsinki.

Immunohistochemistry on Bone Marrow

For immunohistochemistry (IHC) staining, the following antibody was applied on human bone marrow tissue biopsies by using a routine immunoperoxidase technique: GeneTex C20orf186 antibody, rabbit polyclonal to KLH conjugated synthetic peptide derived from human C20orf186. The Betazoid DAB Chromogen Kit (BioCare Medical) was used as described in manufacturer's recommendations.

Platelets separation from whole blood

Platelets were recovered from PrP samples of above-mentioned healthy donors, and then they were treated with and without $CaCl_2$ 22mM for 40 minutes at 37°C. After the treatment, the platelets were centrifuged at 8000 rpm for 8 minutes and both the supernatant for the next ELISA and the pellet for the following Western-blot were recovered. Afterwards, a part of the PrP in basal conditions was used for immunofluorescence. To obtain platelets from whole blood, a first centrifuge was carried out at 2200 rpm for 20 minutes without brake. After the centrifuge, Tyrode's buffer (Sigma-Aldrich) was added to the recovered PrP in a 1:1 ratio and another centrifuge was performed at 500 g for 15 minutes without brake. Subsequently, the supernatant was removed and the pellet was resuspended in free RPMI and treated with $CaCl_2$ 22mM and with the human recombinant LAV of BPIFB4 protein (rhLAV) at the concentration of 18 ng/mL for 40 minutes at 37°C. A centrifuge at 13000 g for 5 minutes was performed and after being recovered the supernatant was harvested and then used for the following ELISA.

Platelets count

Differentiated parental, EMPTY-, WT- and LAV-MEG-01 cells were counted by using an automatic cell counter (LUNA Automated Cell counter, logos) and two cell fractions were considered: platelet-like particles (PLPs, Ø 1-3 μm) and megakaryocytes (Ø 16-35 μm)**.** The ratio between MEG-01 cells and PLPs was carried out.

Immunofluorescence on PrP

PrP was diluted to 0,5% in Tyrode's buffer and centrifuged at 3000 g for 10 minutes to obtain the platelets. Afterwards, the platelets were resuspended in Tyrode's buffer, loaded into a cytofunnel and spotted onto the slide through the Cytospin (CENTURION-Scientific Limited) at 1200 rpm for 5 minutes. Platelets were fixed with 4% formaldehyde for 10 minutes at room temperature and washed three times with PBS (Gibco®, Thermo Fisher Scientific). Platelets were blocked and permeabilized using PBS with 5% Bovine Serum Albumin (PanReac AppliChem) amd 0,005% saponin for 30 minutes at room temperature. Cells were incubated overnight at 4°C with the following IgG primary antibodies' mix: customized rabbit polyclonal anti-BPIFB4 (purchased from CliniSciences S.r.l.-Guidonia Montecelio – Italy; 1:100 in PBS 2,5% goat serum) and mouse polyclonal anti-P-selectin (Santa Cruz, 1:100 in PBS 2,5% horse serum). The next day, three washes of 10 minutes with PBS were carried out followed by a 30-minutes incubation at RT in the dark with the following secondary antibodies' mix: Alexa Fluor 488-conjugate anti-mouse IgG (Vector Laboratories, 1:200 in PBS) and DyLight 549-conjugated anti-rabbit IgG (Vector Laboratories, 1:200 in PBS). Platelets were washed three times with PBS and nuclei were stained with DAPI (1:100 in PBS) for 20 minutes at room temperature in the dark. After five washes, slides were glycerol-mounted and images were acquired by using a confocal laser-scanning fluorescence microscope TCS SP5 (Leica Microsystems).

Immunofluorescence on parental undifferentiated and differentiated MEG-01

Undifferentiated MEG-01 cells were harvested from flask. $\approx 4x10^5$ cells were diluted in PBS, loaded into a cytofunnel, centrifuged at 300 rpm for 6 minutes through the Cytospin (CENTURION-Scientific Limited) and spotted onto slides. Instead, after PMA-TPO pre-treatment, differentiated MEG-01 cells were seeded onto a 4-well culture chamber slide (Sartstedt). After drawing up the medium, three washes with PBS were carried out to remove suspended cells. Both undifferentiated and

differentiated MEG-01 cells were fixed with 4% formaldehyde for 10 minutes at room temperature and washed three times with PBS. Cells were blocked and permeabilized using PBS with 5% BSA and 0,005% saponin for 30 minutes at room temperature. Cells were incubated overnight at 4°C with the customized IgG primary rabbit polyclonal anti-BPIFB4 (purchased from CliniSciences S.r.l.-Guidonia Montecelio – Italy, 1:100 in PBS 5% goat serum). The next day, three washes of 10 minutes with PBS were carried out followed by a 30-minutes incubation at RT in the dark with the DyLight 549-conjugated anti-rabbit IgG (Vector Laboratories, 1:200 in PBS). Cells were washed three times with PBS and nuclei were stained with DAPI (1:100 in PBS) for 20 minutes at room temperature in the dark. After five washes, slides were glycerol-mounted and images were acquired by using a confocal laser-scanning fluorescence microscope TCS SP5 (Leica Microsystems).

Enzyme-linked immunosorbent assay (ELISA)

BPIFB4 plasma levels were determined using Human Long palate, lung, and nasal epithelium carcinoma-associated protein 4 (C20orf186) ELISA kit (Cusabio CSBYP003694HU) following the manufacturer's protocol. Briefly, the PrP from genotyped healthy donors, the plasma of anti-platelets treated mice and supernatants of platelets extracted from whole blood and treated with $CaCl_2$ were incubated for 2 hours at 37 °C in the coated assay microplate. After removing any unbound substances, a biotin-conjugated antibody specific for C20orf186 was added to the wells and incubated for 1 hours at 37 °C. After washing, avidin-conjugated horseradish peroxidase (HRP) was added to the wells and incubated for 1 hours at 37 °C. Following a wash, the substrate solution was added, and consequent color development was stopped. The optical density was measured at 450 nm.

Western Blotting

Megakaryocytes from mouse bone marrow and platelets from PrP were washed with PBS (Gibco®, Thermo Fisher Scientific), harvested, and lysed in ice-cold RIPA lysis buffer (50 mM Tris-HCl, 150 mM NaCl, 0.5% Triton X-100, 0.5% deoxycholic acid,

10 mg/mL leupeptin, 2 mM phenylmethylsulfonyl fluoride, and 10 mg/mL aprotinin). After centrifugation at 13000 rpm for 20 minutes at 4°C, in order to remove cell debris, proteins were quantified. About 30 μg of proteins were separated on 10% SDS-PAGE at 90 V for 1 hour and at 120 V for another hour and then transferred to a nitrocellulose membrane. After blocking with 5% non fat dried milk powder (PanReacAppliChem) in Tris-buffered saline containing 0.1% Tween-20 (TBST) for 1 hour at room temperature, the membranes were incubated overnight with the following primary antibodies: customized BPIFB4 (purchased from CliniSciences S.r.l.-Guidonia Montecelio – Italy) and β-actin (Abcam #4990 mouse mAb 1:50000). Immunodetection of specific proteins was carried out with horseradish peroxidase-conjugated donkey anti-rabbit IgG (Bio-Rad), using the enhanced chemiluminescence (ECL) system (Thermo Fisher Scientific) according to the manufacturer's instructions and then exposed to X-ray films (Thermo Fisher Scientific). Western-blot data were analyzed using Photoshop software to determine the optical density (OD) of the bands. The OD readings of protein were expressed as a ratio relative to β-actin.

Flow cytometry analysis

PBMCs of treated mice were stained with mAb against mouse CD86 (PO3.3; Miltenyi Biotec; 1:10), CD206 (C068C2; Biolegend; 1:50), and Ly6C (REA796; Miltenyi Biotec; 1:50). After 30 minutes incubation at 4°C in the dark, cells were washed with staining buffer (PBS 2% fetal serum bovine, 0,01% sodium azide), centrifuged at 1800 rpm for 5 minutes, and resuspended in staining buffer for the FACS analysis. Instead, MEG-01 cells were incubated for 30 minutes at 4°C in the dark with a primary customized anti-BPIFB4 (purchased from CliniSciences S.r.l.-Guidonia Montecelio – Italy, 1:100); then cells were washed with staining buffer and incubated with secondary PE donkey anti-rabbit IgG (Poly4064; Biolegend; 1:1000) for 30 minutes at +4°C in the dark. At the end of the incubation, the cells were washed as before and then resuspended in staining buffer for the FACS analysis. For each test, cells were analyzed using FACS Verse Flow Cytometer (BD Biosciences).

Aggregometry on diabetic patients and healthy donors PrP

Platelets' aggregation of N=4 diabetic patients as mentioned above was evaluated with the aid of an aggregometer (Platelet Aggregation Profiler-PAP8, BIO/DATA CORPORATION, V 2.0 Optics). For diabetic patients the blood samples in sodium citrate tubes were centrifuged at a low speed to sediment white and red blood cells and to obtain the platelet-rich plasma (PrP). While the aggregometer reached a temperature of 37°C, a small aliquot of PrP was taken and put into specific tubes containing small magnets. The remaining plasma was centrifuged again to obtain platelet-poor plasma, which was used as blank. Afterwards, LAV-BPIFB4 18 ng/ml was added to PrP samples and before reading via PC software connected to the instrument, a platelet activator was also added; in particular, both collagen 0,19 mg/ml (BIO/DATA Corporation) and ADP 20 μM (BIO/DATA Corporation) were used. Therefore, the functioning platelets aggregate and fall to the bottom of the tube. Likewise, the aggregation of healthy donors' platelets treated with high (i.e. 25 mM) and low (i.e. 5mM) glucose concentrations was evaluated with and without rhLAV-BPIFB4 18 ng/ml. The results were expressed as percentage of light transmission measured spectrophotometrically.

Production of lentiviral vectors and transfected EMPTY, WT and LAV MEG-01 cell line

Lentiviral particles (Empty vector, WT- or LAV-BPIFB4) were concentrated by ultracentrifugation (40 000 rpm for 2 h at 4 °C) and stored at −80 °C until immediately prior to use. Lentivirus titration was performed by transducing HEK293T cells with concentrated particles in the presence of 4 μg/ml polybrene and measuring GFP expression after 3 days by flow cytometry. 500.000 MEG-01 cells were plated into 12-well plate in RPMI medium and were infected with empty lentiviral vectors or particles encoding either WT- or LAV-BPIFB4. After 72 h, cells were selected with 1 μg/ml puromycin for 48 h.

Cell lines and culture conditions

MEG-01 (ATCC® CRL-2021) were grown in humidified incubator at 37°C and 5% CO_2 in RPMI-1640 (Gibco®, Thermo Fisher Scientific) supplemented with 10% (v/v) fetal serum bovine (FBS, Gibco®, Thermo Fisher Scientific), 1% (v/v) penicillin-streptomycin (Aurogene), 1% (v/v) MEM non-essential amino acids (MEM NEAA, Gibco®, Thermo Fisher Scientific) and 1% (v/v) sodium pyruvate (Aurogene). Differentiated MEG01 were obtained upon 3 days pre-treatment with phorbol 12-myristate 13-acetate (PMA) 5nM and thrompoietin (TPO) 100 ng/mL. Following the above-mentioned treatment, cells were collected for subsequent assays.

Animal models

The overall objective of our in vivo study was to investigate the role of platelets in the AVV-LAV-BPIFB4 effects. To investigate this, we used C57BL/6 mice from Jackson Laboratories. Mice were randomly assigned to receive injections of either a control IgG or anti-CD42b to deplete circulating platelets after receiving AAV-LAV-BPIFB4 or EMPTY vector, as control. After 72h of platelet depletion mice were harvested, and the blood, lymphoid organs (bone marrow and spleen) and mesenteric aortas collected. The Institutional Animal Care Use Committee of Neuromed Medical Center approved all animal experiments. Mouse colonies were maintained in the animal facility at IRCCS Neuromed, Pozzilli (IS), Italy. At week 10, mice were randomized into two groups and received either control antibody injections (polyclonal non-immune rat immunoglobulins) or a GPIb- alpha antibody (Emfret) injections to deplete circulating platelets (3 μg/g). At sacrifice, mice were anesthetized with ketamine/xylazine, exsanguinated by cardiac puncture, and perfused with PBS, followed by 10% sucrose in PBS.

In vivo gene therapy

Ten-week-old male C57BL/6 mice were anesthetized with 5% isoflurane in 100% O_2 (delivery rate, 5L/min), and placed in dorsal recumbent position on a homoeothermic blanket (N-HB101-S-402) to maintain body temperature at 37°C.

Anaesthesia was maintained with 1% isoflurane in 100% O_2 at 1.5 L/min, administered by means of a facemask connected to a coaxial circuit (Fluovac anaesthetic mask). Vascular surgery was performed with the aid of a microscope at 2–10X magnification. As previously described, femoral arteries were exposed and isolated circumferentially from the inguinal ligament to the knee. To avoid collateral damage to adjacent structures, the artery was carefully separated from associated nerves and veins with fine-tip forceps. After isolation of the arterial segment, a temporary clamp was closed around the proximal end of the artery to temporarily stop the blood flow. Subsequently, the distal end of the femoral artery was permanently occluded to perform a small incision on the superficial wall of the artery, using a syringe connected, through a PE10 – polyethylene tube, with a glass needle tip of 80 microns in diameter, to inject either 50µl of saline containing AAV-GFP or AAV-LAV-BPIFB4 into the femoral artery. Viral titre was 1×10^{13} GC/kg for each experimental condition. After an incubation of 5 minutes, before carefully removing the syringe, we performed a permanent ligation just after the incision, and the clamp on the proximal femoral artery removed to restore femoral blood flow and obtain systemic delivery. As support to the procedure's success, evaluation of GFP revealed the expression of AAV9 (TBG-promoter) into the liver, thus confirming its systemic delivery. Mice remained anaesthetized for 1 h, after which all received 100% O_2 until recovery of righting reflex. Animal groups subjected to either control antibody injections (polyclonal non-immune rat immunoglobulins) or a GPIb- alpha antibody (Emfret) injections (3 µg/g), received a blood injection through caudal vein (tail) after 24h of AAV- delivery. Mice were sacrificed 96h after surgery and vascular gene therapy. Mesenteric and femoral arteries were harvested and placed respectively on pressure and wire system for vascular reactivity studies.

Mice tissue sampling and processing

Plasma and Peripheral Blood Mononuclear Cells (PBMCs) were extracted from whole blood of mice by Ficoll density gradient (Histopaque®-1077, Sigma-Aldrich). Plasma was employed to estimate the BPIFB4 levels dosage while PBMCs were

stimulated *in vitro* with lipopolysaccharide (LPS) at a concentration of 1 μg/ml and then analyzed by flow cytometry. Mouse bone marrow was extracted from the femurs through the flushing method on ice. Femurs were cut at both ends with a sterile blade and bone marrow was flushed out by using a 10 cc syringe filled with RPMI-1640 (Gibco®, ThermoFisher Scientific) supplemented with 2% (v/v) penicillin–streptomycin (Aurogene). Bone marrow-derived cell suspensions were harvested into a tube to let debris deposit. Cell suspension was transferred into a new tube and centrifuged at 1900 rpm for 5 min at room temperature. After discarding the supernatant, cells were incubated to CD61 MicroBeads of Miltenyi Biotec to obtain $CD61^+$ and $CD61^-$ cells. In particular, after determining cells number, magnetic labeling was carried out following manifacturer's istructions, as well as the magnetic separation perfomed through an LS column with an appropriate MACS Separator. Unlabeled cells were also collected. The cells thus obtained were lysed in RIPA lysis buffer (50 mM Tris-HCl, 150 mM NaCl, 0.5% Triton X-100, 0.5% deoxycholic acid, 10 mg/mL leupeptin, 2 mM phenylmethylsulfonyl fluoride, and 10 mg/mL aprotinin and the extracted proteins were used for the following Western-blot.

Statistical Analysis

In all experiments shown, statistical analysis was performed using the GraphPad prism 6.0 software package for Windows (GraphPad software). For each type of assay or phenotypic analysis, the data obtained from multiple experiments were calculated as mean ± SD and analyzed for statistical significance using appropriate tests. In the analysis of variance (ANOVA) for multiple comparisons, p-values < 0.05 were considered significant; * $p < 0.05$, ** $p < 0.01$, and *** $p < 0.001$.

Discussion

In the past few years it was extensively documented the peculiar activity of a longevity-associated variant (LAV) of bactericidal/permeability-increasing fold-containing family-B-member-4 (BPIFB4) protein encoded by a four-SNP haplotype of BPIFB4 gene in promoting health/longevity; this was achieved by the enhancement of the vascular cell homeostasis, the postischemic revascularization and progenitor cell mobilization, the advantageous remodeling of the heart, by blunting the disease-associated inflammatory circuits and mainly by counterbalancing age-related immunological and cardiovascular impairment. These helped to partially explain the health status of Long-Living-Individuals (LLIs) and their LAV-BPIFB4 homozygous genotype enrichment.

Here it was discovered that platelet depletion in the wild-type mice model completely abolished the vasculoprotective action of LAV-BPIFB4 on endothelial function and blunted the monocyte skewing through which LAV-BPIFB4 guarantees protection against inflammatory stimuli, such as LPS. The platelet-dependence observed in vivo (Fig. 5.3) is consistent with the characterization of platelets as a new reservoir of huge amount of BPIFB4 protein (Fig. 5.1). This is expected as platelets fulfil a much wider role in health and disease through the storage and the release of a wide range of biologically active substances including the panoply of growth factors, chemokines and cytokines essential for the innate immune response and combat infection (viruses, bacteria, microorganisms). Further, activated platelets intervene in the propagation of major diseases. They are cellular players in atherosclerosis and related diseases, in cardiomyopathy and diabetic pro-thrombotic phenotype. Accordingly, it was discovered that LAV-BPIFB4 halts the increased atherogenic process observed in high-fat diet treated-ApoE-/-animals. Treatment with LAV-BPIFB4 reduces inflammatory markers, skewing splenic macrophages towards an anti-inflammatory M2 phenotype, and increases athero-protective interleukins, thereby leading to an improvement of endothelial vasorelaxation and reduction of plaque formation. Moreover, the LAV-BPIFB4 gene improves endothelial and

cardiac function in obese mice with type 2 diabetes mellitus and platelets could likely be the means of LAV-BPIFB4 therapeutic action. The results indicate that BPIFB4 is increased in platelets in the basal state and following Ca2+ activation its levels are not raised like other mediators, which may have suggested de novo protein synthesis, but it is properly secreted (Fig. 5.1). Concerning this, even though it was didn't check the BPIFB4 transcript in platelets, the presence of the protein in the highly specialized Megakaryocytes (MKs), suggest that platelet BPIFB4 can derive from those cytoplasmic proteins and granules that precursor cells accumulate for platelet function (Fig. 5.2). The primary site of generation of MKs is the bone marrow niche where the expression level of BPIFB4 after AVV-LAV-BPIFB4 infection have been well documented also in previous published reports. The BPIFB4 immunoreactivity not only of MKs but also of common myeloid progenitors in Fig. 5.2A may suggest the existence of a stem cell expressing BPIFB4. These observations along with the ability of LAV-BPIFB4 to trigger the mobilization of endothelial progenitor cells may warrant a future analysis of BPIFB4 in stem cell compartment. Here it was showed that CD61+ cells from murine BM are mainly enriched for BPIFB4 compared to CD61- counterpart. CD61 (β3 integrin), a membrane-bound glycoprotein that forms a heterodimer with CD41 (GP IIb) to form the GPIIb/IIIa (CD41/CD61) complex, is used to identify blasts with megakaryocytic differentiation or other megakaryocytes. Consistently, it was also found BPIFB4 to be highly expressed in MEG-01 cells (Fig. 5.2B), a megakaryoblastic leukemia cell line. It can be differentiated in vitro by phorbol-12-myristate-13-acetate (PMA) treatment to produce platelet-like-particles (PLPs). In the differentiated cells the shift from cytoplasm to nucleus of BPIFB4 expression, may occur in order to regulate gene expression or simply to participate in endoreplication leading to polyploidy and subsequent formation of pro-platelets processes. Indeed surface FACS analysis of terminally differentiated MEG-01 (Fig. 5.2C) showed a significant upregulation of BPIFB4 signal on the membrane from the breakdown of which platelets are usually generated. As consequence it was reported a significant increase in PLPs formation in LAV-BPIFB4 MEG-01 cells compared to WT-BPIFB4 MEG-01 counterpart (Fig.

5.2D). How the effects of genotype can influence the degree of platelets release both in vitro (Fig. 5.2D) and in vivo (Fig. 5.1E) remains to be examined. In mice stressed with anti-platelet antibody, the pre-exposure of the whole animal to LAV-BPIFB4 gene therapy enhanced the survival of MK in vitro and/or increased the percentage of CD41+ cells among the primary BM cells after long term stimulation with Thrombopoietin (TPO). Future efforts to underpin the role of LAV-BPIFB4 in megakaryopoiesis may be useful for human applications to prevent or treat the thrombocytopenia that would otherwise occur in several disease conditions. Even though association studies between platelet phenotype and LAV-BPIFB4 genotype in disease are ongoing, here it was suggest an effector role for platelets in achieving healthy effects of LAV-BPIFB4 ensuring elevated plasma level of circulating BPIFB4 (Fig. 5.3B), which is considered a prognostic biomarker in prolonging health-span, in determining COVID-19 and coronary artery disease (CAD) severity, and the degree of carotid stenosis and intima media thickness in human patient cohorts. To understand the functional role of BPIFB4 in platelets, it was stimulated platelets with rhLAV-BPIFB4. Surprisingly, LAV-BPIFB4 exclusively inhibited in vitro the hyper aggregation of human platelets in hyperglycemic conditions (Fig. 5.4B-C) and displayed antithrombotic activity in vivo (Fig. 5.5). In conclusion, of 300 proteins released by platelets, some of which are well characterized whilst many are not, it was reported that BPIFB4 in auto-paracrine manner, displayed a regulatory role of the coagulation. In future, additional studies may clarify its activity as a factor of the platelet secretory artillery to reduce platelets activation itself and if LAV-BPIFB4 genotype and/or BPIFB4 levels may correlate with platelet activity in several disease conditions. This will open the way to the translation approach to use LAV-BPIFB4 recombinant protein to finely tune platelet bio-functions and rescue the pro-thrombotic phenotype associated to several cardiovascular disease (CVDs).

Conclusion

Studying the LAV-BPIFB4 protein in different contexts has added new insights into its pleiotropic effects. In long-lived subjects, an association between circulating protein levels and monocyte distribution was confirmed in favor of the patrolling phenotype, precursor of reparative M2 macrophages. The associative description of data does not allow conclusively that the skewed monocyte profile contributes to the longer life expectancy of the studied LLIs, however, this study is the first to identify a major monocyte subset in individuals who reach extreme ages (>95 years old). It is reasonable to assume that high levels of circulating BPIFB4 assist with M2 polarization, thereby providing an innate immunity background that is supportive of disease resistance and the control of inflammatory responses. In the context of cellular senescence, a widespread phenotype in aging, the protein has been shown to play a role in the modulation and regulation of cellular haemostasis. Data in vitro e in mouse model, suggest a new senotherapeutic action of LAV-BPIFB4, which may provide a valuable therapeutic tool to control aging and reduce its pathophysiological disorders, such as cardiovascular disease. The context of senescence can also be decisive in cancer therapy, since numerous therapeutic approaches exploit cell replication for their efficacy. In senescent GBM cells, LAV enhances their sensitivity to temozolomide and reduces select T cells' senescence. A potential mechanism explaining the improved response to TMZ may be the downregulation of MDR levels by LAV-BPIFB4 on the surface of ETP-treated senescent cells. In fact, it has been demonstrated that the inhibition and control of the MDR complex correlate with an increased sensitivity of GBM to temozolomide. The pre-treatment of TMZ-exposed glioma cells with LAV-BPIFB4 may restore these cells' ability to reenter the cell cycle and contribute to the TMZ-induced toxicity, as evidenced by the higher apoptotic rate produced by LAV-BPIFB4 co-treatment. It is important to note that, despite the need to deeply analyze the mechanisms underlying these effects, it is likely that in the future treatment with LAV-BPIFB4, as well as other senotherapeutics, might prove valuable in restoring therapy-sensitivity and a proper

immune surveillance. An additional pathological context, not directly related to senescence or immunity, such as neurodegeneration, has also been studied using a Huntington's disease model (HD). The evidence supports the specificity of the positive relationship between LAV-BPIFB4 and the SFD-1/CXCR4 signaling pathway in HD. Due to the dual effect of LAV-BPIFB4 on striatum and immune surveillance, it was proposed that gene transfer or alternatively the use of human recombinant proteins of LAV-BPIFB4 in presymptomatic HD carriers could be a promising strategy to delay HD onset or improve HD symptoms in the future. Due to the fact that platelets are primary mediators of the innate immune response and are capable of contrasting infections, it was investigated whether this blood figurative element played a role in immunomodulatory processes of the BPIFB4 protein. Among the 300 proteins released by platelets, some of which are well characterized and others not, it was reported that BPIFB4 can control coagulation in an auto-paracrine manner. Additional studies in the future may clarify its role as a factor of the platelet secretory artillery to reduce platelet activation itself and if levels of LAV-BPIFB4 correlate with platelet activity in several diseases. The development of LAV-BPIFB4 recombinant protein will permit the translation of a therapeutic approach for fine-tuning platelet biofunctions and reversing the prothrombotic phenotype associated with several cardiovascular diseases (CVDs).

Bibliography

Introduction

1. Muñoz-Espín D, Serrano M. Cellular senescence: from physiology to pathology. Nat Rev Mol Cell Biol. 2014 Jul;15(7):482-96. doi: 10.1038/nrm3823. PMID: 24954210.
2. Lehmann J, Baar MP, de Keizer PLJ. Senescent Cells Drive Frailty through Systemic Signals. Trends Mol Med. 2018 Nov;24(11):917-918. doi: 10.1016/j.molmed.2018.09.003. Epub 2018 Oct 3. PMID: 30292430.
3. Di Micco R, Krizhanovsky V, Baker D, d'Adda di Fagagna F. Cellular senescence in ageing: from mechanisms to therapeutic opportunities. Nat Rev Mol Cell Biol. 2021 Feb;22(2):75-95. doi: 10.1038/s41580-020-00314-w. Epub 2020 Dec 16. PMID: 33328614; PMCID: PMC8344376.
4. Kumari R, Jat P. Mechanisms of Cellular Senescence: Cell Cycle Arrest and Senescence Associated Secretory Phenotype. Front Cell Dev Biol. 2021 Mar 29;9:645593. doi: 10.3389/fcell.2021.645593. PMID: 33855023; PMCID: PMC8039141.
5. Kirkland JL, Tchkonia T. Cellular Senescence: A Translational Perspective. EBioMedicine. 2017 Jul;21:21-28. doi: 10.1016/j.ebiom.2017.04.013. Epub 2017 Apr 12. PMID: 28416161; PMCID: PMC5514381.
6. Montella F, Lopardo V, Cattaneo M, Carrizzo A, Vecchione C, Ciaglia E, Puca AA. The Role of BPIFB4 in Immune System and Cardiovascular Disease: The Lesson from Centenarians. Transl Med UniSa. 2021 Dec 23;24(1):1-12. doi: 10.37825/2239-9754.1029. PMID: 36447743; PMCID: PMC9673912.
7. Malavolta M, Dato S, Villa F, De Rango F, Iannone F, Ferrario A, et al. LAV-BPIFB4 associates with reduced frailty in humans and its transfer prevents frailty progression in old mice. Aging (Albany NY) 2019;11:9220. https://doi.org/10. 18632/aging.102209.

8. Britto CJ, Cohn L. Bactericidal/Permeability-increasing protein fold-containing family member A1 in airway host protection and respiratory disease. Am J Respir Cell Mol Biol 2015;52:525e34. https://doi.org/10.1165/rcmb.2014-0297RT.
9. Dang Z, Avolio E, Thomas AC, Faulkner A, Beltrami AP, Cervellin C, et al. Transfer of a human gene variant associated with exceptional longevity improves cardiac function in obese type 2 diabetic mice through induction of the SDF-1/ CXCR4 signalling pathway. Eur J Heart Fail 2020;22:1568e81. https://doi.org/10.1002/ejhf.1840.
10. Spinetti G, Sangalli E, Specchia C, Villa F, Spinelli C, Pipolo R, et al. The expression of the BPIFB4 and CXCR4 associates with sustained health in long-living individuals from Cilento-Italy. Aging (Albany NY) 2017;9:370e80. https://doi.org/10.18632/aging.101159.
11. Di Pardo A, Ciaglia E, Cattaneo M, Maciag A, Montella F, Lopardo V, et al. The longevity-associated variant of BPIFB4 improves a CXCR4-mediated striatum-microglia crosstalk preventing disease progression in a mouse model of Huntington's disease. Cell Death Dis 2020;11:546. https://doi.org/ 10.1038/s41419-020-02754-w.
12. Villa F, Malovini A, Carrizzo A, Spinelli CC, Ferrario A, Maciąg A, et al. Serum BPIFB4 levels classify health status in long-living individuals. Immun Ageing 2015;12:27. https:// doi.org/10.1186/s12979-015-0054-8.

Chapter I

1. Caruso C, Aiello A, Accardi G, Ciaglia E, Cattaneo M, Puca A. Genetic signatures of centenarians: implications for achieving successful aging. Curr Pharm Des. (2019) 25:4133–8. doi: 10.2174/1381612825666191112094544
2. Connelly MA, Otvos JD, Shalaurova I, Playford MP, Mehta NN. A novel biomarker of systemic inflammation and cardiovascular disease risk. J Transl Med. (2017) 15:219. doi: 10.1186/s12967-017-1321-6

3. Franceschi C, Garagnani P, Vitale G, Capri M, Salvioli S. Inflammaging and 'Garb-aging'. Trends Endocrinol Metab. (2017) 28:199–212. doi: 10.1016/j.tem.2016.09.005
4. Emerging Risk Factors Collaboration, Kaptoge S, Di Angelantonio E, Loit was G, Pepys MB, Thompson SG, et al. C-reactive protein concentration and risk of coronary heart disease, stroke, and mortality: an individual participant metaanalysis. Lancet. (2010) 375:132–40. doi: 10.1016/S0140-6736(09)61717-7.
5. Thomas G, Tacke R, Hedrick CC, Hanna RN. Nonclassical patrolling monocyte function in the vasculature. Arterioscler Thromb Vasc Biol. (2015) 35:1306–16. doi: 10.1161/ATVBAHA.114.304650.
6. Nahrendorf M, Swirski FK, Aikawa E, Stangenberg L, Wurdinger T, Figueiredo JL, et al. The healing myocardium sequentially mobilizes two monocyte subsets with divergent and complementary functions. J Exp Med. (2007) 204:3037–47. doi: 10.1084/jem.20070885.
7. Olingy CE, San Emeterio CL, Ogle ME, Kriegere JR, Bruce AC, Pfau DD, et al. Non-classical monocytes are biased progenitors of wound healing macrophages during soft tissue injury. Sci Rep. (2017) 7:447. doi: 10.1038/s41598-017-00477-1.

Chapter II

1. Borgoni S, Kudryashova KS, Burka K, de Magalhães JP. Targeting immune dysfunction in aging. Ageing Res Rev. 2021;70:101410. https://doi.org/10.1016/j. arr.2021.101410
2. Katsyuba E, Romani M, Hofer D, Auwerx J. NAD+ homeostasis in health and disease. Nat Metab. 2020;2:9–31. https://doi.org/10.1038/s42255-019-0161-5
3. Yousefzadeh MJ, Flores RR, Zhu Y, Schmiechen ZC, Brooks RW, Trussoni CE, et al. An aged immune system drives senescence and ageing of solid

organs. Nature. 2021;594:100–5. https://doi.org/10.1038/s41586-021-03547-7

4. Chini CCS, Peclat TR, Warner GM, Kashyap S, Espindola-Netto JM, de Oliveira GC, et al. CD38 ecto-enzyme in immune cells is induced during aging and regulates NAD+ and NMN levels. Nat Metab. 2020;2:1284–304. https://doi.org/10.1038/ s42255-020-00298-z
5. Puca AA, Carrizzo A, Spinelli C, Damato A, Ambrosio M, Villa F, et al. Single systemic transfer of a human gene associated with exceptional longevity halts the progression of atherosclerosis and inflammation in ApoE knockout mice through a CXCR4-mediated mechanism. Eur Heart J. 2020;41:2487–97. https://doi. org/10.1093/eurheartj/ehz459
6. Frederick DW, Loro E, Liu L, Davila A Jr, Chellappa K, Silverman IM, et al. Loss of NAD homeostasis leads to progressive and reversible degeneration of skeletal muscle. Cell Metab. 2016;24:269–82. https://doi.org/10.1016/j.cmet.2016.07.005

Chapter III

1. Weller, M.; van den Bent, M.; Tonn, J.C.; Stupp, R.; Preusser, M.; Cohen-Jonathan-Moyal, E.; Henriksson, R.; Le Rhun, E.; Balana, C.; Chinot, O.; et al. European Association for Neuro-Oncology (EANO) guideline on the diagnosis and treatment of adult astrocytic and oligodendroglial gliomas. Lancet Oncol. 2017, 18, e315–e329.
2. Eggert, T.; Wolter, K.; Ji, J.; Ma, C.; Yevsa, T.; Klotz, S.; Medina-Echeverz, J.; Longerich, T.; Forgues, M.; Reisinger, F.; et al. Distinct Functions of Senescence-Associated Immune Responses in Liver Tumor Surveillance and Tumor Progression. Cancer Cell 2016, 30, 533–547
3. Aasland, D.; Götzinger, L.; Hauck, L.; Berte, N.; Meyer, J.; Effenberger, M.; Schneider, S.; Reuber, E.E.; Roos, W.P.; Tomicic, M.T.; et al. Temozolomide Induces Senescence and Repression of DNA Repair Pathways in

Glioblastoma Cells via Activation of ATR–CHK1, p21, and NF-kB. Cancer Res. 2019, 79, 99–113

4. Kosar, M.; Bartkova, J.; Hubackova, S.; Hodny, Z.; Lukas, J.; Bartek, J. Senescence-Associated heterochromatin foci are dispensable for cellular senescence, occur in a cell type- and insult-dependent manner and follow expression of p16(ink4a). Cell Cycle 2011, 10, 457–468.
5. Campisi, J.; d'Adda di Fagagna, F. Cellular senescence: When bad things happen to good cells. Nat. Rev. Mol. Cell Biol. 2007, 8, 729–740
6. Tivnan, A.; Zakaria, Z.; O'Leary, C.; Kögel, D.; Pokorny, J.L.; Sarkaria, J.N.; Prehn, J.H. Inhibition of multidrug resistance protein 1 (MRP1) improves chemotherapy drug response in primary and recurrent glioblastoma multiforme. Front. Neurosci. 2015, 9, 218.
7. Dossena, M.; Ferrario, A.; Lopardo, V.; Ciaglia, E.; Puca, A.A. New Insights for BPIFB4 in Cardiovascular Therapy. Int. J. Mol. Sci. 2020, 21, 7163
8. Pereira, B.I.; Devine, O.P.; Vukmanovic-Stejic, M.; Chambers, E.S.; Subramanian, P.; Patel, N.; Virasami, A.; Sebire, N.J.; Kinsler, V.; Valdovinos, A.; et al. Senescent cells evade immune clearance via HLA-E-mediated NK and CD8+ T cell inhibition. Nat. Commun. 2019, 10, 2387.
9. Ruth, A.C.; Roninson, I.B. Effects of the multidrug transporter P-glycoprotein on cellular responses to ionizing radiation. Cancer Res. 2000, 60, 2576–2578.

Chapter IV

1. Reiner, A., Dragatsis, I. & Dietrich, P. Genetics and neuropathology of Huntington's disease. Int. Rev. Neurobiol. 98, 325–372 (2011).
2. Dayalu, P. & Albin, R. L. Huntington disease: pathogenesis and treatment. Neurol. Clin. 33, 101–114 (2015).
3. Ransohoff, R. M. A polarizing question: do M1 and M2 microglia exist? Nat. Neurosci. 19(8), 987–991 (2016).

4. Nakagawa, Y. & Chiba, K. Diversity and plasticity of microglial cells in psychiatric and neurological disorders. Pharmacol. Ther. 154, 21–35 (2015).
5. Palpagama, T. H., Waldvogel, H. J., Faull, R. L. M. & Kwakowsky, A. The Role of Microglia and Astrocytes in Huntington's Disease. Front. Mol. Neurosci. 12, 1–15 (2019).
6. Crotti, A. & Glass, C. K. The choreography of neuroinflammation in Huntington's disease. Trends Immunol. 36, 364–373 (2015).
7. Trettel, F. et al. Dominant phenotypes produced by the HD mutation in STHdh(Q111) striatal cells. Hum. Mol. Genet. 9, 2799–2809 (2000)
8. Konstantinova, I. M., Tsimokha, A. S. & Mittenberg, A. G. Role of proteasomes in cellular regulation. Int. Rev. Cell. Mol. Biol. 267, 59–124 (2008).
9. Chafekar, S. M. & Duennwald, M. L. Impaired heat shock response in cells expressing full-length polyglutamine-expanded huntingtin. PLoS ONE 7, e37929 (2012).

Chapter V

1. Karen Y. Stokes and D. Neil Granger. Platelets: a critical link between inflammation and microvascular dysfunction. Physiol 590.5 (2012) pp 1023–1034 doi:10.1113/jphysiol.2011.225417
2. Ali RA, Wuescher LM, Worth RG. Platelets: essential components of the immune system. Curr Trends Immunol. 2015;16:65-78. PMID: 27818580; PMCID: PMC5096834.
3. F. Mussano et al. Cytokine, chemokine, and growth factor profile of platelet-rich plasma. Platelets, doi:10.3109/09537104.2016.1143922
4. Voja Pavlovic et al. Platelet Rich Plasma: a short overview of certain bioactive components. Open Med. 2016; 11: 242-247 doi 10.1515/med-2016-0048

5. Klinger MHF. Anat. Embryol. 1997; 196:1. [PubMed: 9242884]
6. Yeaman MR. Clin. Inf. Dis. 1997; 25:951.
7. Hamzeh-Cognasse H, Damien P, Chabert A, Pozzetto B, Cognasse F, Garraud O. Front. Immunol. 2015; 6:82. [PubMed: 25767472]
8. Ali RA, Wuescher LM, Worth RG. Platelets: essential components of the immune system. Curr Trends Immunol. 2015;16:65-78. PMID: 27818580; PMCID: PMC5096834.
9. Kraemer BF, Campbell RA, Schwertz H, Cody MJ, Franks Z, Tolley ND, Kahr WHA, Lindemann S, Seizer P, Yost CC, Zimmerman GA, Weyrich AS. PLoS Pathogens. 2011; 7:e1002355. [PubMed: 22102811]
10. Britto CJ, Cohn L. Bactericidal/Permeability-increasing protein fold-containing family member A1 in airway host protection and respiratory disease. Am J Respir Cell Mol Biol 2015;52:525e34. https://doi.org/10.1165/rcmb.2014-0297RT.
11. Dang Z, Avolio E, Thomas AC, Faulkner A, Beltrami AP, Cervellin C, et al. Transfer of a human gene variant associated with exceptional longevity improves cardiac function in obese type 2 diabetic mice through induction of the SDF-1/CXCR4 signalling pathway. Eur J Heart Fail 2020;22:1568e81. https://doi.org/10.1002/ejhf.1840.
12. Spinetti G, Sangalli E, Specchia C, Villa F, Spinelli C, Pipolo R, et al. The expression of the BPIFB4 and CXCR4 associates with sustained health in long-living individuals from Cilento-Italy. Aging (Albany NY) 2017;9:370e80. https://doi.org/10.18632/aging.101159
13. Di Pardo A, Ciaglia E, Cattaneo M, Maciag A, Montella F, Lopardo V, et al. The longevity-associated variant of BPIFB4 improves a CXCR4-mediated striatum-microglia crosstalk preventing disease progression in a mouse model of Huntington's disease. Cell Death Dis 2020;11:546. https://doi.org/10.1038/s41419-020-02754-w.

14. Villa F, Malovini A, Carrizzo A, Spinelli CC, Ferrario A, Maciąg A, et al. Serum BPIFB4 levels classify health status in long-living individuals. Immun Ageing 2015;12:27. https:// doi.org/10.1186/s12979-015-0054-8.
15. Villa F, Carrizzo A, Spinelli CC, Ferrario A, Malovini A, Maciag A, et al. Genetic analysis reveals a longevity-associated protein modulating endothelial function and angiogenesis. Circ Res 2015;117:333e45. https://doi.org/10.1161/ CIRCRESAHA.117.305875.
16. Ciaglia E, Montella F, Lopardo V, Scala P, Ferrario A, Cattaneo M, et al. Circulating BPIFB4 levels associate with and influence the abundance of reparative monocytes and macrophages in long living individuals. Front Immunol 2020; 11:1034. https://doi.org/10.3389/fimmu.2020.01034.
17. Puca AA, Carrizzo A, Spinelli CC, Damato A, Ambrosio M, et al. Single systemic transfer of a human gene associated with exceptional longevity halts the progression of atherosclerosis and inflammation in ApoE knockout mice through a CXCR4-mediated mechanism. Eur Heart J 2020;41:2487e97. https://doi.org/10.1093/eurheartj/ehz459.